Reactions to Specific Comments from Anonymous Referee #1

General comments:
This manuscript deals with the nature of the particle size distribution of stratospheric sulfate aerosols. The main motivation is to improve assumptions on the aerosol scattering phase function required to retrieve aerosol extinction coefficients from satellite limb-scatter measurements. The study presents a re-analysis of balloon-borne measurements of the aerosol size distribution with optical particle counters. Specifically, two different size distributions (uni-modal log-normal and gamma distributions) are used to model the observed cumulative distributions. The manuscript is interesting,presents relevant new information and should eventually be published in my opinion. The paper is very well written and generally easy to follow. There are several points I ask the authors to consider. Specific comments (often minor) are listed below. In addition, I have one more general comment:

The analysis is based on a more limited number of OPC channels than previous analyses of the measurements. In particular, the channels corresponding to large particle sizes are now not considered. These channels provided evidence for a second mode of the particle size distribution, even under background conditions. The second mode is now entirely neglected and the reader wonders, whether the authors now believe that the second mode does not really exist? I think this aspect should be explicitly addressed in the paper. The small number of large particles contributes substantially to the overall aerosol scattering signal and will probably also have a non-negligible effect on the scattering phase function. This is particularly relevant, because the gamma distribution systematically underestimates the number of particles for the largest size bin (top right panel of Fig. 6.)

Response: The fitting of two uni-modal distributions to OPC and OPC$_{nsb}$ data was motivated by Figure A2 of (Chen et. al 2018), who fitted four Bi-modal lognormal distributions (BMLN) to OPC$_{nsb}$ data measured on 12 April 2000 for altitude 20 km. All four fits had a similar AE of approximately 2.4, but each had different coarse mode fraction (CMF). These four BMLN distribution fits to the OPC data differed significantly from each other in the radius range between 0.01 $\mu\mathrm{m}$ to 0.1 $\mu\mathrm{m}$ and these differences resulted from the gaps in the OPC size bins that limited the ability of the fits to be constrained. All four fits captured the larger particles very well but the resulting phase functions differed from each other because of the overestimation or under estimation of the particles between 0.01 and 0.1 $\mu\mathrm{m}$. The two gamma distributions are in good agreement with each other especially within the particle radius range of 0.01 $\mu\mathrm{m}$ to 0.1 $\mu\mathrm{m}$ but both systematically failed to capture the number concentration of the largest bin. Since the actual phase function is not known, it is possible that either of the phase functions from the UMLN or gamma may be right.

Also it should be noted that most of the OPC measurements associated with the OMPS measurement period lack measurable signals in the larger bins, especially in the 20-25 km altitude range that is most relevant for the current OMPS retrieval assessments (Chen et. al 2018). Therefore, these measurements do not provide a clear argument for the presence of larger particles in those cases. For cases that DO have a measurable signal for large aerosol bins, the signal remains much lower than in the smaller size bins. So (in a global, weighted fit like was performed), it may be appropriate for the fit to the data at the largest size bins to be very poor (relative to the the much higher signals in the smaller bins).

Specific comments:

1- Page2, line 31 "using Mie theory (Deirmendjian,1969)" I suggest citing the original paper by Mie here (Mie,1908)
Response: The line has been updated to "using Mie theory (Mie,1908)"

2- Page 2, same line "Here we make the assumption that the aerosol particles in the stratosphere are spherical" If Mie theory is used this assumption is implicitly made anyway. Perhaps this could be explicitly stated.

Response: This sentence has been revised to: "Theoretically, the $P_a(\Theta)$ is calculated from the aerosol size distribution (ASD) using Mie theory (Mie, 1908), generally assuming that the aerosol particles in the stratosphere are spherical and homogeneous."

3- Page3, line 61: "to correct the ASD"
Response: This sentence has been revised to read: "to retrieve the ASD"

4- Page3, line 66: "and found out that even if the particles were assumed to be spherical" I don't understand this part of the sentence, because, (a) if Mie theory is used the particles are implicitly assumed to be spherical anyway, (b) if the HG phase function is used no explicit assumptions on the particle shape have to be made, right?
Response: The statement has been revised, it now reads: "Some techniques that have been used to model the $P_a(\Theta)$ are by computing it using the Henyey-Greenstein phase function (H-G) (Henyey and Greenstein, 1941; Ernst, 2013; Grams, 1981) or the modified Henyey-Greenstein phase function (MH-G) (Irvine, 1965; Cornette and Shanks, 1992) with a precise asymmetry factor g, which is the average cosine of the scattering angle weighted by the phase function. The shortcomings of using these functions to approximate the real Mie phase function were demonstrated by Toublanc (1996) for two cases. When the radius of the particle was ten times smaller than the wavelength, the H-G phase function failed to produce the shape of the real Mie phase function in comparison to that of the MH-G. By contrast, for a particle of radius that was comparable to the wavelength, both functions failed to reproduce the lobe patterns of the real Mie phase function."

5- Page4, lines108/109: coagulation is certainly also an important process for the growth of stratospheric aerosols.
Response: Coagulation is also an important stratospheric aerosol formation process and it has been included in the sentence, which now reads:
'A multimodal distribution can be used to represent coexisting "nucleation" , "coagulation", and "accumulation" modes after a volcanic eruption. The nucleation mode is associated with new particle formation from sulfur vapor which quickly coagulate to form larger particles (Hamill et al., 1997), and the accumulation mode associated with particle growth by condensation of the vapor on the existing particles (Steele and Turco, 1997).'

6- Page6, line 162 and equation(3): if O_i is already the "frequency" in each size bin, i.e. normalized to the total number of observations, then the multiplication of the expected probability values ζ_i with n in equation (3) is not required, is it? O_i corresponds to a probability then, and so does ζ_i
Response: O_i is the "frequency" in each size bin. It is normalized by dividing by "n". Rearranging the equation will then lead to the "n" in the denominator being squared (which was omitted). Equation (3) has now been updated squaring "n" in the denominator. On the other hand, if O_i is defined as the normalized "frequency" in each size bin, then the multiplication of the expected probability values ζ_i with "n" in the equation would not be required.

7- Page7, line 185: "The LPC data consists of 20 months of measurements" Table 2 lists more than 20 months.
Response: This sentence has been corrected to read: "The LPC data consists of 27 months of measurements" to correspond to the number of months listed in Table 2.

8- Page,10 Figure 1: I think it would be quite interesting for the reader to see plots of the non-cumulative versions of the gamma and UMLN distributions for these cases.
Response: Figure 1 has been updated to include non-cumulative versions of the gamma and UMLN distributions for the two cases shown.

9- Same Figure: It is also worth mentioning in the text that the ASDs differ substantially for radii > 300 nm. At 600 nm or so the difference one order of magnitude.

Response: The text has been updated to include the above suggestion:

"The two ASDs tend to diverge beginning at radii greater than 300 nm and differ substantially at approximately 600 nm, where aerosol concentrations are below the minimum detectable concentrations, and there these differences can reach one order of magnitude."

10- Page 11, line 242: "This is shown in Figure 5, where one observes a considerable change in the magnitude of the phase function, especially in the back-scattering directions ($\Theta \geq 90°$) for this X value" I don't think this statement is correct. Looking at the Figure, the phase function for X=1 is almost constant for scattering angles > 90 degrees. Perhaps you intended to make another point?

Response: The above statement has been rephrased to read:

"The phase function for X = 3 shows a forward peak and is nearly constant for scattering angles ($\Theta \geq 70°$). When there are no measurements between the 0.01 and 0.15 μm bin sizes, then the particle concentration within this range is estimated by the function used to fit the data. Errors in estimating the number of particles within this range by the function used for fitting the data will lead to uncertainties in the phase function as shown by the X = 1 plot in Figure 5."

11- Page 12, caption Figure 5: "increase .. complexity of the phase function" The complexity (e.g. for X=10) is mainly due to the fact that a mono disperse aerosol is assumed here. If you assumed a UMLN or a gamma distribution then the oscillations will be damped.

Response: The caption of Figure 5 has been revised to read: "Mie phase functions of a monodisperse aerosol for different values of the size parameter X derived with a refractive index of 1.33. The increasing asymmetry and complexity (e.g. for X=10) of the phase functions with increasing X is due to the use of a monodisperse aerosol. The oscillations observed are damped when the phase functions are computed for an ensemble of aerosols that are assumed to have a UMLN or gamma distribution. The phase functions are shown for the range of scattering angles that are observed by OMPS, SCIAMACHY and OSIRIS."

12- Page 13, Figure 6 and related discussion in the main test: I certainly agree that the differences between the OPC-like and LPC-like fits are smaller for the gamma distribution than the UMLN distribution. However, both gamma distributions systematically underestimate the number of in the largest bin. If larger bins would be considered this low bias would probably be even larger. So the two gamma distributions are in good agreement, but they are also both systematically wrong. Perhaps their phase functions deviate even more from the actual phase functions compared to the phase function based on the UMLN distribution? Looking at the χ^2, the UMLN distribution without the extra measurement still show the best performance. I am not asking for any more analysis here, but I think it should be clearly stated that the gamma distributions fail to capture the OPC measurements for the largest sizes, which will lead a systematic error in the derived phase functions.

Response: "OPC-like" has been changed to OPC$_{nsb}$ and "LPC-like" has been changed to OPC: "nsb" stands for no small bin .

There was no arbitrary decision to ignore measurements from the largest bin when the fits were made. Thus the systematic underestimation of the concentration of the largest bin by the gamma distribution fits was not deliberate as the same can be seen for the UMLN fit (red line). Because the actual phase function is not known, it is possible that the phase functions derived from the gamma or the UMLN distribution functions may be the right one.

This has been stated in the text as "The failure of both gamma distributions to capture the OPC measurements for the largest bin size for the case shown in Figure 6 could lead to a systematic error in the derived phase functions."

13- Page 14, line 287: "The gamma distribution does not have the same tendency to over estimate the larger particles" This is now different from the earlier analysis of the OPC/LPC measurements, where the gamma distribution systematically underestimated the large particles.
Response: These are the CARMA microphysical model outputs at Wyoming and these are different from the OPC/LPC measurements made at the same location.

14- Page 16, Figure 7: "The blue data points" I can't identify blue points on my printout.
Response: The size of the blue dots has been increased.

15- Page 18, line 325: "Additionally, it has been shown that whenever OPC-like concentration measurements are made, the gamma distribution is the best distribution to be fitted" I don't agree with this statement, because χ^2 for the OPC-like measurements is significantly smaller for the UMLN distribution than the gamma distribution. Please rephrase this statement to eliminate this apparent contradiction. As mentioned above, the difference between the gamma-fits for the OPC-like and LPC-like measurements are admittedly very small, but the gamma distribution systematically under estimates the measurements for radii > 300 nm. Since the large particles dominate the scattering signal, they will have a non-negligible effect on the phase function. It may even be possible that the OPC-like UMLN distribution yield a phase function that agrees best with the actual phase function.
Response: Figure 6 is a comparison of the fits made with the inclusion of a small bin (OPC) to one with no small bin (nsb) OPC_{nsb} measurements. On this figure, the χ^2 value for OPC UMLN distribution fit is 0.0135 and that of gamma distribution fit is 0.0101. This shows that the χ^2 for the gamma fit is somewhat less than that of the UMLN fit. This is in agreement with the statement:

"Additionally, it has been shown that when the same LPC concentration measurements are fit without using the 0.092 $\mu\mathrm{m}$ bin, the gamma distribution provides a some what better fit because of its insensitivity to particles between 0.01 $\mu\mathrm{m}$ and 0.1 $\mu\mathrm{m}$ range when compared to the UMLN distribution; however the gamma distribution in both cases underestimates the concentrations of the larger particles, which may be quite important depending on the wavelength of interest"

16- Page 18, general comment on the conclusion: the 2nd mode reported in earlier study is now entirely neglected. The earlier OPC measurements showed indications for the second mode even under background conditions. I guess this measurements are still valid- they are also based on more channels at larger radii. It would be good if the authors would comment on how to treat the second mode in future studies. The large particles with radii of several 100 nm may have a substantial impact on overall scattering properties and the phase function of stratospheric sulfate aerosols.
Response: During background conditions, Deshler et al. (2003) have in some cases used a bimodal lognormal (BMLN) particle size distribution to achieve the best fit to the OPC measurements made by the in situ optical counters. However, with limb scattering geometry this BMLN size distribution is not possible because six (or five when the data points are normalized) independent pieces of information at each altitude will be needed to describe the BMLN distribution, but at altitudes greater than 20 km, OPC measurements mostly provide four data points. This makes it impossible to fit a bimodal distribution.

Also, we agree that particles with radii larger than 100 nm may have a substantial impact on the overall scattering properties and the phase functions of the stratospheric sulfate aerosol during volcanically active or periods with pyro CB activity. But most of the limb radiance measurements made by OMPS in the last seven years is devoid of any large volcanic activity sufficient enough to inject aerosols into the stratosphere and are mostly considered as background condition.
In the future, we hope to compare the phase functions derived from multi-modal aerosol size distributions.

Typos etc,:
1- Page 2, line 7: "Philippines,1991" -> "Philippines, 1991"

Response: This has been corrected.

2- Page 2, line 35: ",longitude" -> ", longitude"
Response: This has been corrected.

3- Page 3, line 58: "occulation" -> "occultation"
Response: This has been corrected.

4- Page 3, line 58: "was began" -> "was begun"
Response: This has been corrected.

5- Page 3, line 59: I think "that" in "that provided" can be omitted.
Response: This has been corrected.

6- Page 3, line 67: "calculations .. was" -> "calculations .. were"
Response: This has been corrected.

7- General comment on spelling of “Angström”: sometimes you use "A" as the first letter,sometimes "Å". I think the latter is correct and should perhaps be used throughout the manuscript.
Response: This has been updated everywhere in the manuscript.

8- Page 3, line 75, equation (1): "nm" can be omitted here (4 occurrences)
Response: This has been corrected for all occurrences.

9- Page 4, line 86: "on measurements from Laramie, Wyoming optical particle counter (OPC) measurements"
Response: This sentence has been corrected to read "on data from Laramie, Wyoming optical particle counter (OPC) measurements"

10- Page 4, line 98: "by (Deepak .." and next line "or (Hinds" Wrong cite command used (\citep -> \cite}
Response: This has been corrected.

11- Page 4, line 10: "Sparc" -> "SPARC"
Response: This has been corrected.

12- Page 7, line 183: "following (Kovilakam" \citep -> \cite
Response: This has been corrected.

13- Page 9, line 226: add space after "shape parameter"
Response: This has been corrected.

14- Page 12, line 260: ".This" -> ". This"
Response: The correction has been made.

15- Page 14, lines 264 and 266: \citep -> \cite
Response: This has been corrected.

16- Page 18, line 309: "in the along the" -> "along the"
Response: The correction has been made.

17- Page 23, line 471: "Sparc" -> "SPARC"
Response: The correction has been made

18- Same line: add space in "(eds.),SPARC"
Response: The correction has been made.

Reactions to Specific Comments from Anonymous Referee #2

In the present paper, authors try to answer the question which shape of the aerosol size distribution (ASD) is it better to use for stratospheric aerosols. In the paper, two shapes of the stratospheric ASD were taken into consideration, namely, unimodal lognormal (UMLN) and gamma-distribution. Both distributions were fitted to the data from Optical Particle Counters (OPC) and the CARMA model. The quality of the fits was compared using the χ^2 criterion. Based on this comparison, it was concluded that gamma-distribution provides more realistic aerosol phase function (APF) than UMLN distribution. The latter application is particularly important for the aerosol extinction retrievals from the limb scatter instruments. While the research itself is thoroughly conducted and convinces the reader that gamma-distribution fits better than UMLN OPC and CARMA model data, the part about the use of gamma-distribution in the limb scatter retrievals is completely missing. There is a long discussion in the manuscript about the importance of the APF for limb scatter instruments (which is absolutely true), and there are nice studies showing the APF from the gamma-distributions. However, the authors did not show any application of the improved APF in the retrievals. Based on this major issue, the following can be suggested:

- authors include some additional study, where the improvement of the limb retrievals with the corrected APF is shown;
- or authors revise the manuscript in a way that they, for example, leave the recommendation to fit OPC data with gamma-distribution rather than with UMLN during the background aerosol loading.

While both revisions will be sufficient to publish the manuscript in AMT, I would suggest going with the first one. Otherwise, the purpose for the APF discussion should be justified differently.

Response: A parallel study by (Chen et al. 2018) have compared retrieved aerosol extinctions using the OMPS/LP V1.0 (bimodal lognormal), V1.5 (gamma distribution) derived from the CARMA model output to the extinction profile derived from SAGE III (on the International Space Station). The results show an improvement in the V1.5 extinctions to within 10% at altitudes 19-29 km. The authors of the paper are including this information and referencing the above paper.

Specific Comments:
1- P.2, L.1: Maybe it would be good to add to the cited works the newer studies? E.g., Ivy, D. J., Solomon, S., Kinnison, D., Mills, M. J., Schmidt, A., and Neely, R. R.: The influence of the Calbuco eruption on the 2015 Antarctic ozone hole in a fully coupled chemistry-climate model, Geophysical Research Letters, 44, 2556–2561, 2017
Response: The citations have been updated to include (ivy et al. 2017). Also the effect on the ozone hole enhancement by the presence of volcanic aerosols associated with Calbuco has been mentioned in the same paragraph.

2- P.2, L.27: Here it is important to mention such sources of stratospheric aerosols as wildfires smoke (see for example Khaykin et al. (2018), https://doi.org/10.1002/2017GL076763) and SO_2 from Asian pollution (e.g., Randel et al. (2010), DOI:10.1126/science.1182274).
Response: Other sources of stratospheric aerosols from wildfire smoke and SO_2 from Asian pollution have been mentioned and the Khaykin et al. (2018) and Randel et al. (2010) have been cited.

3- P.2, L. 28 and 33: Is there a difference between $P_a(\Theta)$) and APF? If there is, then it should be better highlighted. If there is not, then just one abbreviation should be used throughout the manuscript.
Response: There is no difference between $P_a(\Theta)$ and APF. Only $P_a(\Theta)$ will be used to subsequently represent the Stratospheric Aerosol Phase function.

4- P.3, L.70: It would be nice to mention here, and in Table 1 SCIAMACHY aerosol extinction algorithm V1.4 (see Rieger et al. (2018)).
Response: SCIAMACHY has been mentioned in both places.

5- P.3, Eq.(1): The above-mentioned products provide aerosol extinction at one wavelength, so the Eq. (1) can not be used for them to calculate Ångström exponent, because the second extinction coefficient is missing. However, the Eq. (1) is generally absolutely correct and can be used to calculate Ångstöm exponent using the ASD and Mie theory. It would be better to add the sentence before, that the formula is correct for the general case. Otherwise, the reader gets the impression that Ångström exponent is computed from the products
Response: The sentence has been revised to include that the extinction of the two wavelengths are derived using the ASD and Mie theory. "The figures also display for each fit the Ångström exponent (AE) that was computed using Equation (1), where λ_1 and λ_2 are 525 nm and 1020 nm respectively.

6- P.4, L.103: Firstly, for all three publications cited here UMLN was used. Secondly, they all used certain assumptions (simply because spaceborne measurements do not provide enough pieces of information). I think it should be mentioned here
Response: The cited publications have been updated to include Loughman et al.(2018), which used BMLN aerosol size information for the extinction retrievals. Also it has been mentioned that space-borne measurement do no provide enough pieces of information.

7- P.6. L.172: I think it should be explained why the particles in size range between 0.05 and 0.1 $\mu\mathrm{m}$ are so important in this study. Smaller particles also scatter solar radiation, and the next sentence says that OPC measurements include particles with radii greater than 0.01 $\mu\mathrm{m}$. Therefore, the importance of this particular size range should be justified.
Response: In a case study (see Figure A1 of Chen et al., 2018), four bimodal lognormal size distributions were fitted to the same data set which did not have a measurement between 0.05 µm and 0.1 µm. The differences observed in the resulting phase functions were due to the differences of the fits at that radius range because all four fits captured the larger bins very well. This shows the importance of aerosol particles within the radius range 0.05 $\mu\mathrm{m}$ and 0.1 $\mu\mathrm{m}$.

8- P.12, L.258-261: It is hard to understand the purpose of the whole Section 3.2 and its main message. Is the purpose to show that gamma-distribution is less sensitive to the particles smaller than 0.1 µm? Then it is a good result for OPC fit, and it should be highlighted. However, for the limb instruments, this fit might be relatively useless then Coarse resolution of the data on particles smaller then 0.1 µm does not mean that there are no particles of this size and that they will not influence the "real" distribution. Or is there a misunderstanding of the Section?
Response: This section tests the sensitivity of the two unimodal distributions to determine which distribution would accurately predict the amount of particles within the particles radius range of 0.01$\mu\mathrm{m}$ and 0.1$\mu\mathrm{m}$ during the period when there are no measurements within this particle radius range (no small bin (nsb) or OPC_{nsb}) and when there is at least a measurement within that range (OPC).

Also the conclusion has been rephrased to read:
"The conclusion drawn from this comparison is that the phase functions calculated with the gamma distributions with and without the small bin are comparable to each other to within 10% as compered to those of the UMLN distribution. This signifies that the gamma distribution is relatively insensitive to the addition of an intermediary bin between 0.05 $\mu\mathrm{m}$ and 0.1 $\mu\mathrm{m}$, whereas the UMLN distribution is quite sensitive to this additional information."

9- P.14, L.272: Firstly, it is better to use μm instead of the nm here, because it might confuse the reader. Secondly, I assume that the bins are not equally distributed over the presented size range and that there is information on small particles. Were there attempts to fit gamma-distribution to the "raw" output of CARMA model to see how this distribution behaves with more information on the particles smaller than 0.1 μm? Or this question is irrelevant because the purpose of Section 3.2 was wrongly interpreted?
Response: First, nm has been converted to μm. Secondly, The CARMA model "raw" outputs were used because they provide enough information on smaller particles smaller than 0.1 μm, and for this study these model outputs were subsetted into the OPC measurement bins to find out which of the two uni modal distributions was the best fit to this model output. The conclusion drawn from section 3.2 is to use the gamma distribution to fit OPC_{nsb} data. This section also shows that the gamma distribution is the best fit to the CARMA model outputs. A table showing the distribution of the aerosol size bins used in the CARMA model has been added.

In our next study we plan to fit the gamma distribution to all the "raw" outputs of the CARMA model.

10- P.15, L.303-305: If I understand correctly, CARMA is planned to be used for OMPS retrieval,which should be explicitly mentioned.
Response: The plan to use phase functions derived from the CARMA model outputs in OMPS retrievals has been stated in the manuscript.

11- P.18, L.334-349: As it was said in the general comments, the part about the space borne instruments is absolutely missing. Thus, it should be either removed and reformulated for OPC measurements, or some real studies using limb instruments should be done
Response: A parallel study by (Chen et al. 2018) have compared retrieved aerosol extinctions using the OMPS/LP V1.0 (bimodal lognormal), V1.5 (gamma distribution) derived from the CARMA model output to the extinction profile derived from SAGE III (on the International Space Station). The results show an improvement in the V1.5 extinctions to within 10% at altitudes 19-29 km. The authors of the paper are including this information and referencing the above paper.

Technical corrections:

1- P.1, L.1-2: The first sentence in the abstract leaves an impression that OPC provided measurements only from 2008-2017, which is not true. See e.g., Deshler et al. 2003.
Response: it has been clarified in the abstract that this is a subset of the total data since measurements have been taking place since 1971 (Deshler et al. 2003).

2- P.3, L.28: There is not much sense to shorten "solar occultation" to "SO" since it is used just once. If the authors want to save some space, it is better to shorten "Figure"to "Fig." and "Equation" to "Eq.".
Response: Noted

3- P.4, L.98-99: The citation here should be done as "Deepak and Box (1982) or Hinds(1982)".
Response: Noted

4- P.4, L.101: Sparc better spelled as SPARC.
Response: Noted

5- P.6, L.151: Here I think is a typo, and 6 data points were meant.
Response: Because we are using the coarse mode fraction (CMF), which is the ratio of the coarse mode concentration to the total, the number of parameters reduces from 6 to 5.

6- P.8, L.212: Maybe "percentile" should not be in italics?
Response: Noted.

7- P.14, L.282: Maybe leave χ^2 here instead "chi-squares"?
Response: Noted

8- P.18, L.308: I think citations should be listed chronologically.
Response: Noted

Reactions to Specific Comments from Anonymous Referee #3

This paper presents an analysis of the suitability of log-normal and gamma distributions to the particle size measurements from in situ OPC balloon flights. The authors motivate this work based on the implications that the fitted distribution has on the derived aerosol scattering phase function that is required in the radiative transfer forward modeling for limb scattering retrievals of aerosol extinction.

The results have merit and the study is well conducted; however, I completely agree with the major issue raised by Referee #2. The study needs to include a quantitative assessment of the impact these results have on the aerosol retrievals. Reporting the difference in phase functions, as the study currently stands, is of limited use, but with some additional work to show the impact on the retrievals, it becomes potentially quite important. One aspect to consider for example is that the forward scattering peak that the authors sometimes choose to cut off the phase function figures can be quite important with multiple scattering and high albedo. In line with this comment, I think the authors should put this study more deeply in the context of the Chen et al., 2018. There are similarities and those should be discussed in detail in light of the new results. Finally, the work would be more broadly useful if wavelengths other than $675\mathrm{nm}$ were also studied (SCIAMACHY and OSIRIS use $750\mathrm{nm}$ for example)

Response: Chen et al. 2018, have conducted a parallel study where they compared the retrieved aerosol extinction profiles from the OMPS/LP using the V1.0 (bimodal lognormal distribution) and V1.5 (gamma distribution) retrieval algorithms to the extinction profiles derived from SAGE III (on the International Space Station). The results obtained, indicated an improvement in the V1.5 extinction profiles to within 10% at altitudes 19-29 km. The authors of the paper are including this information and referencing the above paper.

In our next study, we plan to include other wavelengths greater than $675\mathrm{nm}$.

Minor Comments:
1- Mixed use of APF and P_a in the text for the aerosol phase function. Choose one.
Response: There is no difference between $P_a(\Theta)$ and APF. Only $P_a(\Theta)$ will be used to represent the Stratospheric Aerosol Phase function.

2- Abstract line 11: what does “stable” mean?
Response: The sentence contain the word "stable" has been removed.

3- Abstract last sentence: The exclusion of certain bins is too specific for the nature of the rest of the abstract (cannot be understood without a lot more detail from the paper)
Response: Noted. The last part of the Abstract has been rephrased.

4- Introductory paragraph should probably contain some motivating statement about the impact of several moderate volcanic eruptions over the last decade.
Response: This has been noted and we have added a statement about the impact of moderate volcanic eruptions.

5- Line 32: what does “homogeneous” mean? i.e. there is still a size distribution of particle sizes; also, the refractive index should be for hydrated sulfuric acid, and should be stated and referenced
Response: The word "homogeneous" is used in this line to mean "the particles have the same properties throughout".The

refractive index has been stated for hydrated sulfuric acid and referenced.

6- Lines 65-68: Quantify “sufficient” and “high precision”; this statement needs more detail
Response: More details have been included to elaborate on the statements made by Toublanc (1996).

7- Line 69: Bourassa et al., ACP, 2012 is the reference for OSIRIS version 5.0
Response: Noted

8- Line 72: Size distribution parameters for OMPS v1.0 and v1.5 should be stated, possibly included in Table 1 somehow
Response: The size distribution parameters of OMPS v1.0 and v1.5 have been included in Table 1.

9- Line 73: Use of Angstrom exponent should be motivated; this statement is out of place at the moment
Response: A motivational statement has been included.

10- Equation 1: Typesetting with units is strange
Response: The units have been removed from the equation.

11- Line 159: “similarity in appearance” needs quantification; otherwise this is not a helpful statement
Response: The statement "similarity in appearance” has been deleted from the text.

12- Line 163: No brackets on equation numbers
Response: Noted and corrected.

13- Table 2: Is this information necessary?
Response: This information is necessary to show the reader the months in which measurement were made each year and also the frequency of measurements throughout the period considered (2008 - 2017).

14- Figure 1: Green text on figures is hard to read
Response: A darker shade of green has been used on this figure.

15- Line 218: something wrong with the wording here
Response: The word "taking" has been replaced with "taken".

16- Line 223: It doesn’t follow that the phase functions agree for scattering angles greater than 20 degrees “because the fits of the two distributions overlap"
Response: The statement “because the fits of the two distributions overlap" has been removed.

Relevant Changes

The following changes have been made in the manuscript:

1. The abstract has been rewritten.

2. Table 1 has been updated to include the aerosol size distribution parameters that are used by the various OMPS versions. Also included are the ASD parameters of SCIAMACHY (V1.4).

3. The terms "OPC-like" and and "LPC-like" are no longer being used in the manuscript. Instead the term "OPC-like" has been changed to OPC$_{nsb}$ and "LPC-like" has been changed to OPC: "nsb" stands for no small bin.

4. Equation 2 has been changed from

$$N(>r) = \sum_{i=1}^{n} \int_{r}^{\infty} \frac{N_i}{\sqrt{2\pi} ln\sigma_{mi}} \exp\left(\frac{-ln^2[x/r_{mi}]}{2ln\sigma_{mi}}\right) d\, lnx$$

   to include counting efficiency functions (CEFs)

$$N_{ch} = \int_{0}^{\infty} \left[\sum_{i=1}^{n} \frac{N_i}{\sqrt{2\pi} \bullet ln[\sigma_{mi}]} \exp\left(\frac{-ln^2[x/r_{mi}]}{2 \bullet ln^2[\sigma_{mi}]}\right)\right] CEF_{ch}(x) d\, ln(x).$$

5. Added plots comparing the phase functions of Gam$_{nsb}$ to UMLN$_{nsb}$ and Gam to UMLN to Figure 6.

6. Table 3 has been included in the manuscript to show the distribution of the 22 aerosol size bins for the radii of the particles that are used in the CARMA model.

7. Equation 7 has been update from

$$RD\ (\%) = \left(1 - \frac{P_u}{P_g}\right) \times 100\%$$

   to

$$RD\ (\%) = \left(\frac{P_g - P_u}{P_u}\right) \times 100\%$$

   The relative diffrences are now being calculated in reference to the UMLN phase function (P_u) instead of the gamma phase function (P_g). This has resulted in the change in the magnitudes of the relative differences in Figure 9.

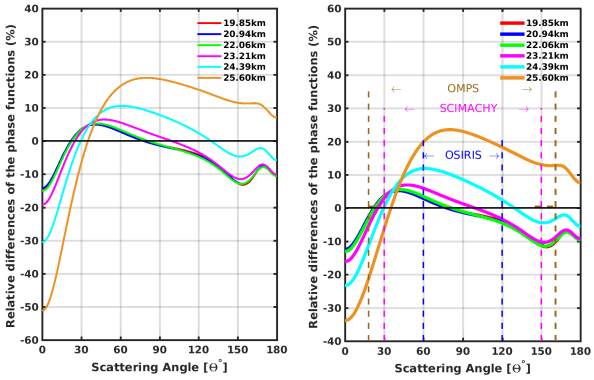

. The figure on the left hand side has been updated to the one on the right hand side.

A comparison of lognormal and gamma size distributions for characterizing the stratospheric aerosol phase function from OPC measurements

Ernest Nyaku[1], Robert Loughman[1], Pawan K. Bhartia[2], Terry Deshler[3], Zhong Chen[4], and Peter R. Colarco[2]

[1]Center of Atmospheric Science, Hampton University, Hampton
[2]NASA Goddard Space Flight Center, Greenbelt, Maryland, 20771, USA
[3]Department of Atmospheric Science, University of Wyoming, Laramie, Wyoming
[4]Science Systems and Applications, Inc. (SSAI), 10210 Greenbelt Road, Suite 600, Lanham, Maryland 20706, USA

Correspondence: Ernest Nyaku (ernest.nyaku@hamptonu.edu)

Abstract.

A series of in situ measurements made by optical particle counters (OPC) at Laramie, Wyoming provides size-resolved stratospheric aerosol concentration data [..[1]]over the period 1971 - 2018. A subset of these data covering the period of 2008-2017 [..[2]]is analyzed in this study for the purpose of assessing the sensitivity of the stratospheric aerosol phase function to the aerosol size distribution (ASD) model used to fit the measurements. The two unimodal ASD models investigated are the uni-modal lognormal (UMLN) and gamma distribution models, with the minimum χ^2 method employed to assess how well each ASD fits the measurements. The aerosol phase function ([..[3]]$P_a(\Theta)$) for each ASD is calculated using Mie theory, and is compared to the [..[4]]$P_a(\Theta)$ derived from the Community Aerosol and Radiation Model for Atmospheres (CARMA) sectional aerosol microphysics module. Comparing the χ^2 values for the fits at altitudes of 20 and 25 km shows that the UMLN distribution better represents the OPC measurements[..[5]][..[6]]; however, the gamma distribution [..[7]]also fits the CARMA model results better than the UMLN model, when the CARMA model results are [..[8]]subsetted into the OPC measurement bins[..[9]][..[10]]

. Comparing phase functions derived from the UMLN distribution fit to OPC data with gamma distributions fit to CARMA model results at the location of the OPC measurements shows a satisfying agreement ($\pm$5%) within the scattering angle range of limb sounding satellites. This uncertainty is considerably larger if the CARMA data are fit with a UMLN.

[1]removed: for the period of
[2]removed: . These data are
[3]removed: APF
[4]removed: APF
[5]removed: . The importance of data at aerosol radius below 0.1
[6]removed: is also demonstrated: When these data are not available from OPC measurements
[7]removed: provides a more stable derived APF. The gamma distribution
[8]removed: binned to mimic
[9]removed: (and therefore measurements between 0.05 and 0.1
[10]removed: are excluded) .

1 Introduction

The presence of aerosol particles in the stratosphere has significant impact on atmospheric dynamics, atmospheric chemistry, and climate by altering the amount of radiation that reaches the Earth's surface, as research over the past few decades has shown [..[11]](Kremser et al., 2016; Ivy et al., 2017). These aerosols form a layer of liquid droplets that are a mixture of sulfuric acid (H_2SO_4) and water (H_2O), discovered by Junge in 1960 (Junge et al., 1961). They can cool the Earth's surface and troposphere by scattering incoming short-wave radiation and warm the lower stratosphere by absorbing outgoing long-wave radiation (Robock, 2000; Kravitz et al., 2011; Ridley et al., 2014). These aerosols [..[12]]in the stratosphere act as condensation nuclei for polar stratospheric clouds (PSCs), which provide a surface for heterogeneous chlorine activation and denitrification processes leading to ozone depletion (McCormick et al., 1995; Andreae and Crutzen, 1997; Solomon, 1999). Model simulations have shown that the Antartic ozone hole was enhanced due to the addition of volcanic aerosols to the lower stratosphere that were associated with the eruption of Calbuco in 2015 (Ivy et al., 2017). The main sources of the stratospheric aerosols as summarized by Kremser et al. (2016) are from sulfur dioxide (SO_2) and carbonyl sulfide (OCS), which are both oxidized to sulfuric acid. OCS originates from marine sources and is transported by convection into the tropical stratosphere from the troposphere. Through large volcanic eruptions, SO_2 is also injected directly into the stratosphere leading to an increased aerosol concentration that lasts for several years as was observed after the eruptions of El Chichón (Mexico, 1982) and Pinatubo (Philippines, 1991). The past 20 years has not experienced any large volcanic eruptions, but during this period the stratospheric aerosol load has been controlled by "moderate" but recurring volcanic eruptions that have been reported to be a primary source of the enhancement of global aerosol content (Vernier et al., 2011; Berthet et al., 2017). These moderate volcanic plumes are injected between 18-20 km in the lower stratophere, and through the upwelling branch of the Brewer-Dobson circulation, they are lofted into the mid-stratosphere up to 25 km altitude in about one year (Vernier et al., 2011). Other sources of stratospheric aerosols are from pyrocumulonumbus firestorms that inject large amounts of combustion products and smoke into the stratosphere (Fromm et al., 2010; Khaykin et al., 2018) and from the transport of SO_2 from the surface to deep into the stratosphere through the Asian monsoon whose circulation provides an effective avenue for pollution from Asia, Indonesia, and India to enter the global stratosphere (Randel et al., 2010).

The stratospheric aerosol phase function $P_a(\Theta)$ describes the angular distribution of the scattered solar radiation and it depends on the size, shape, and refractive index of the aerosol. The value of the phase function for a given scattering angle is proportional to the probability that an incident photon will be scattered in a particular direction. [..[13]]Theoretically, the $P_a(\Theta)$ is calculated from the aerosol size distribution (ASD) using Mie theory [..[14]](Mie, 1908), generally assuming that the aerosol particles in the stratosphere are spherical and homogeneous[..[15]]. In this study, a refractive index [..[16]]of $1.45 + 0i$ is assumed as appropriate for hydrated sulfuric acid (Palmer and Williams, 1975). An estimate of the actual $P_a(\Theta)$ is

[11] removed: (Kremser et al., 2016)
[12] removed: found
[13] removed: The
[14] removed: (Deirmendjian, 1969). Here we make the assumption
[15] removed: and apply
[16] removed: which is appropriate for sulfuric acid. The aerosol phase function (APF)

needed to [..[17]]interpret limb scatter (LS) measurements [..[18]](Rault and Loughman, 2007; von Savigny et al., 2015), and LIDAR measurements, [..[19]]in order to estimate the aerosol extinction profile needed for the aerosol forcing calculations. The $P_a(\Theta)$ estimate is not needed for satellite measurements which use occultation, which measures extinction directly. The actual ASD varies in space (latitude, longitude, and altitude) and time, but scattering based retrievals rarely include this variation.

The Ozone Mapping and Profiler Suite, Limb Profiler (OMPS/LP) [..[20]](Flynn et al., 2006; Rault and Loughman, 2013; Jaross et al., 2014), the Optical Spectrograph and InfraRed Imaging System (OSIRIS) (Llewellyn et al., 2004) and Scanning Imaging Absorption spectroMeter for Atmospheric CartograpHY (SCIAMACHY) (Bovensmann et al., 1999) are three limb scattering instruments that have been mounted on satellite platforms to measure limb scattered sunlight. These satellite instruments have measured the limb radiance profiles from wavelengths ranging from the UV to the near infrared from which stratospheric aerosol extinction profiles, the standard operational product (for OMPS/LP and OSIRIS) are retrieved. The retrieval of stratospheric aerosol extinction profiles from limb radiance measurements (Rault and Loughman, 2007; Bourassa et al., 2007, 2008; Taha et al., 2011; Ovigneur et al., 2011; Bourassa et al., 2012; Ernst, 2013; von Savigny et al., 2015; Rieger et al., 2015, 2018; Loughman et al., 2018), involves the comparison of measured limb radiance data with simulated radiances that are generated by radiative transfer (RT) models. This approach has also been used to obtain the ASD information of stratospheric aerosol from limb scatter measurements (Malinina et al., 2018).

Several ASDs that are used in the aerosol extinction retrieval algorithms by the various LS instruments are presented in Table 2 of Loughman et al. (2018). In many cases, the assumed size distributions used for the derivation of the phase functions are based on lognormal distribution fits made to the University of Wyoming [..[21]]balloon-borne optical particle counter (OPC) measurements that have been made at different places and times. These fits were made prior to the OPC corrections proposed by Kovilakam and Deshler (2015) and [..[22]]Deshler et al. (2019). The $P_a(\Theta)$s derived from the OPC measurements are used in the computation of the limb radiances, which are then compared to the measured radiances to retrieve the aerosol extinction coefficients. As a result, the retrieved aerosol extinction is related to the $P_a(\Theta)$ employed in the retrieval process. [..[23]]Mie theory shows that the shape of the $P_a(\Theta)$ varies considerably with particle size and refractive index. Thus for spherical sulfuric acid droplets in the stratosphere with a known refractive index, as the particle size increases, the shape of the $P_a(\Theta)$ changes from a simple Rayleigh symmetric phase function to a more complex one with more forward scattering (Boucher, 1998).

A long historical record of stratospheric aerosol monitoring is available from the Stratospheric Aerosol and Gas Experiment (SAGE) solar [..[24]]occultation data. This measurement technique was [..[25]]begun by the Stratospheric Aerosol Measurement

[17] removed: accurately
[18] removed: (von Savigny et al., 2015; Rault and Loughman, 2007), or
[19] removed: to yield extinction estimates, but not
[20] removed: (Jaross et al., 2014; Rault and Loughman, 2013; Flynn et al., 2006)
[21] removed: OPC measurements
[22] removed: Deshler et al. (2018). These APFs
[23] removed: The
[24] removed: occulation (SO)
[25] removed: began

(SAM) and then the SAGE series [..[26]]provided a nearly continuous data record from 1984 -2005 (Russell and McCormick, 1989; McCormick and Veiga, 1992; Thomason et al., 1997). SAGE [..[27]]solar occultation data provides a weak constraint on the ASD through the wavelength dependence of the retrieved aerosol extinction, but cannot be used [..[28]]to uniquely retrieve the ASD (Yue, 1999; Thomason et al., 2008). Due to the lack of global ASD information, different groups have used various techniques to model the $P_a(\Theta)$. [..[29]]Some techniques that have been used to model the $P_a(\Theta)$ [..[30]]are by computing it [..[31]]using the Henyey-Greenstein phase function (H-G) [..[32]](Henyey and Greenstein, 1941; Ernst, 2013; Grams, 1981) or the modified Henyey-Greenstein phase function (MH-G) (Irvine, 1965; Cornette and Shanks, 1992) with a precise asymmetry factor g, which is the average cosine of the scattering angle weighted by the phase function. The shortcomings of using [..[33]]these functions to approximate the real Mie phase function were demonstrated by Toublanc (1996) [..[34]]for two cases. When the radius of the particle was ten times smaller than the wavelength, the [..[35]]H-G phase function failed to produce the shape of the real Mie phase function in comparison to that of the MH-G. By contrast, for a particle of radius that was comparable to the wavelength, both functions failed to reproduce the lobe patterns of the real Mie phase function.

The OSIRIS version 5 [..[36]](Bourassa et al., 2012), the OMPS version 0.5 (Loughman et al., 2015; DeLand et al., 2016) and the SCIAMACHY version 1.4 (Rieger et al., 2018) aerosol extinction retrievals use a single-mode lognormal ASD to model $P_a(\Theta)$, by using the median radii (r_m) and widths (σ) given in Table 1. For both algorithms, $P_a(\Theta)$ does not vary with altitude or location. [..[37]]The recently developed V1 (Loughman et al., 2018) and V1.5 (Chen et al., 2018) OMPS aerosol extinction retrieval use updated bi-modal lognormal and gamma phase functions respectively[..[38]]. The [..[39]]Ångström exponent (AE) [..[40]](Ångström, 1929) is a parameter that captures the variation of the aerosol extinction with wavelength, which provides some indication of particle size. AE values greater than 2 are indicative of small particles (Schuster et al., 2006). The AE

[26] removed: that provided a
[27] removed: SO
[28] removed: uniquely to correct
[29] removed: One technique that has
[30] removed: is
[31] removed: based on the parameters of the
[32] removed: phase function (Ernst, 2013; Grams, 1981)
[33] removed: this function
[34] removed: , who compared the Mie phase function with H-G and modified H-G phase functions for mono-disperse particles and found out that even if the particles were assumed to be spherical,
[35] removed: angular scattering properties could not be approximated to the real phase function with sufficient accuracy if high precision calculations of the phase function was required
[36] removed: (Bourassa et al., 2007) and
[37] removed: (Note that the
[38] removed:)
[39] removed: A
[40] removed: is

is computed using Equation (1), where K_{ext} is the aerosol extinction coefficient [..[41]]derived using the ASD and Mie theory for the two wavelengths of interest (525 nm and 1020 nm).

$$AE = [..^{42}] \frac{-\ln[K_{ext}(\lambda_1)/K_{ext}(\lambda_2)]}{\ln[\lambda_1/\lambda_2]} \quad (1)$$

Table 1. [..[43]] Size distribution parameters used to calculate the aerosol phase functions of the various versions of OMPS[..[44]], OSIRIS v5, and SCIAMACHY v1.4. The Ångström exponent (AE) is derived from Equation (1) using the 525 nm and 1020 nm extinction coefficients (Nyaku, 2016).

Instrument (Data Version)	[..[45]]Distribution	[..[46]]CMF	$r_{m_i}(\mu m)$	σ_i	AE
OMPS (V0.5)	UMLN	-	0.06	1.73	2.34
OMPS (V1.0)	BMLN	0.003	0.09, 0.32	1.4, 1.6	2.01
OMPS (V1.5)	Gamma	-	α =1.8	β =20.5	2.078
OSIRIS (V5)	UMLN	-	0.08	1.60	2.44
SCIAMACHY (V1.4)	UMLN	-	0.11	1.37	2.82

Comparison of the extinction coefficients derived from OPC measurements and SAGE II occultation have shown differences that vary by more than 50% [..[47]]particularly for non-volcanic [..[48]]periods (Kovilakam and Deshler, 2015); however, these differences have been largely eliminated after the calibration error identified by Kovilakam and Deshler (2015) was accounted for in the new method to derive uni/bi-modal lognormal size distributions to fit OPC measurements (Deshler et al., 2019). With the application of this new size distribution retrieval method the extinctions estimated from the OPC measurements agree, within the measurement uncertainty, with both SAGE II and HALOE extinctions nearly throughout the altitude and time periods of these measurements. The aerosol signal in the measured LS radiance at a given tangent height is proportional to the product of the aerosol extinction in that layer and the aerosol phase function at the tangent point provided the path is optically thin. Rieger et al. (2018) have shown that [..[49]]differences in assumed lognormal parameters can induce errors of 30% in the aerosol extinction retrievals for OSIRIS geometries and 50% for SCIAMACHY geometries when the [..[50]]exact AE used for the radiance simulations is applied in the extinction retrievals. The analysis of Rieger et al. (2018) illustrates the importance of the assumed value of $P_a(\Theta)$ for LS retrievals of K_{ext}, and the limitations of using AE alone to estimate the value of $P_a(\Theta)$, whereas the analysis of Deshler et al. (2019) illustrates that closure is achieved between well characterized in situ measurements and solar occultation extinction measurements.

[41] removed: for a particular wavelength

[47] removed: depending on altitude and for a volcanic period and less that 50% on the average for

[48] removed: periods (Kovilakam and Deshler, 2015). Also

[49] removed: the differences in the

[50] removed: correct AE is used . These analyses illustrate

This paper seeks to first show the differences that arise in the computed $P_a(\Theta)$ when different size distribution functions are fitted to the same aerosol concentration measurements. The sensitivity of the derived $P_a(\Theta)$ value to the presence or absence of aerosol concentration information in the aerosol size range of 0.01 μm and 0.1 μm is also explored. Section 2 briefly describes some of the ASDs that have been used in the past to characterize the stratospheric aerosol load and a description of the ASD that is derived from aerosol concentration based on [..[51]]data from Laramie, Wyoming optical particle counter (OPC) measurements using balloon-borne instruments [..[52]](Deshler et al., 2003; Ward et al., 2014; Deshler et al., 2019). Section 3 focuses on a study which is based on the 2008 - 2017 OPC data at the same location by comparing the unimodal lognormal (UMLN) and the gamma distribution fits to this data set. This is done by concentrating on two altitudes 20 km and 25 km and noting the differences between the phase functions and the [..[53]]Ångström exponents of these distributions. The two distributions are then compared to the [..[54]]outputs of the Community Aerosol and Radiation Model for Atmospheres (CARMA) sectional aerosol microphysics module running online in the NASA Goddard Earth Observing System (GEOS) model. We conclude with a summary and recommendations on which distribution to choose depending on what kind of stratospheric aerosol measurements are available.

2 Aerosol Size Distribution

The aerosol size distribution or the particle number density per unit radius is a statistical model used to describe an ensemble of particles. A number of particle distributions such as the Junge power-law (Junge, 1963), the modified gamma (Deirmendjian, 1969) and up to seven lognormal (Davies, 1974) distributions have been used in the past to represent the distribution of aerosols in the atmosphere. A comprehensive description and a comparative presentation of these distributions is given by [..[55]]Deepak and Box (1982) or Hinds (1982).

For the characterization of aerosols in the stratosphere, lognormal (LN) size distributions are commonly used, although other distributions have been tried in the past [..[56]](Toon and Pollack, 1976; Rosen and Hofmann, 1986; SPARC, 2006). A discussion of fitting LN distributions to the aerosol measurements obtained from OPC is given by Horvath et al. (1990). LN aerosol size [..[57]]distribution parameters for stratospheric aerosols [..[58]]have also been been retrieved from LS measurements [..[59]](Rault and Loughman, 2013; Rieger et al., 2014; Malinina et al., 2018; Loughman et al., 2018). The UMLN distribution consists of three parameters: The total aerosol concentration and two parameters that indicate the median radius and width of the ASD. The bimodal lognormal (BMLN) distribution became the favored function for fitting stratospheric aerosol

[51] removed: measurements
[52] removed: (Deshler et al., 2003; Ward et al., 2014)
[53] removed: A
[54] removed: model
[55] removed: (Deepak and Box, 1982) or (Hinds, 1982)
[56] removed: (Rosen and Hofmann, 1986; SPARC, 2006)
[57] removed: information
[58] removed: has
[59] removed: (Rault and Loughman, 2013; Rieger et al., 2014; Malinina et al., 2018)

concentration measurement since the eruption of Mount Pinatubo injected [..[60]]large quantities of sulfur dioxide (SO_2) into the stratosphere (Deshler et al., 2003). [..[61]]A multimodal distribution can be used to represent coexisting "nucleation" , "coagulation", and "accumulation" modes [..[62]]after a volcanic eruption. The nucleation mode is associated with new particle formation from sulfur vapor [..[63]]which quickly coagulate to form larger particles (Hamill et al., 1997), and the accumulation mode associated with particle growth by condensation of the vapor on the existing particles (Steele and Turco, 1997).

[..[64]]

2.1 ASD from Wyoming OPC measurements

Stratospheric aerosol measurements to altitudes above 30 km have been [..[65]]

2.2 [..[66]]

[..[67]]taken from balloon-borne platforms at Laramie, Wyoming since 1971 with [..[68]]a one liter per minute two channel OPC originally developed by Rosen (1964) and then [..[69]]with a modified 10 liter per minute 8 -12 channel counter (Hofmann and Deshler, 1991). The instrument measures the intensity of scattered white light at 25° (Rosen, 1964) and 40° (Hofmann and Deshler, 1991) in the forward direction from single particles passing through the light beam, which is larger than the air sample stream. See Table 1 of Deshler et al. (2003) for the measurement history up to 2003. Mie theory is used to determine aerosol size from the [..[70]]intensity of the scattered light. The size resolved OPC number concentration measurements are then fitted with an assumed functional form for the size distribution to describe the measurements. The measured concentrations are fitted by either a UMLN or a BMLN size distribution at each measured altitude, where the particle concentrations at distinct size bins are fitted with the function defined by Equation (2) [..[71]](Deshler et al., 2019), where the sum is [..[72]]over either $n = 1$ or 2 modes.

[..[73]]

[60] removed: enormous
[61] removed: This led to the model of
[62] removed: , with the former being
[63] removed: and the latter
[64] removed: Since 1991, in-situ stratospheric aerosol concentration measurements using OPCs at Laramie, Wyoming, USA (41°N) at altitudes up to
[65] removed: made with 8 and 12 channel instruments, in contrast to the two channel instruments used earlier (see Table 1 of Deshler et al. (2003) for the complete measurement history). The data since 1991 are fit with either unimodal or bimodal lognormal size distributions, depending on which of these distributions minimizes the error with the data. When a second mode is apparent in the data, it generally represents those particles which are moving from the accumulation mode to the coarse mode, and thus is more common at lower altitudes.
[66] removed: ASD from Wyoming OPC measurements
[67] removed: Stratospheric aerosol measurements have been taken at
[68] removed: the use of an OPC which was
[69] removed: modified by Hofmann and Deshler (1991)
[70] removed: amount
[71] removed: (Deshler et al., 1993, 2003)
[72] removed: either over

Prior to the analysis of Deshler et al. (2019), Equation (2) was used without including the channel dependent counting efficiency function (CEF_{ch}) (Deshler et al., 1993, 2003).

$$N_{ch} = \int_0^{\infty} \left[\sum_{i=1}^{n} \frac{N_i}{\sqrt{2\pi} \bullet \ln[\sigma_{mi}]} \exp\left(\frac{-\ln^2[x/r_{mi}]}{2 \bullet \ln^2[\sigma_{mi}]} \right) \right] CEF_{ch}(x) d\ln(x). \quad (2)$$

This distribution assumes that the measured concentrations are normally distributed with respect to the logarithm of the radius for each mode of the distribution. While the OPCs in use since 1991 employ 8 [..[74]]to 12 aerosol channels, the number of usable measurements decreases as the concentration of the larger particles decreases below detection thresholds. A minimum of four size resolved concentration measurements are required to fit a bimodal distribution. The fifth measurement is obtained from the measurement of the total aerosol population using a condensation nucleus counter (Campbell and Deshler, 2014). The sixth measurement is obtained from the first channel with no aerosol counts, providing [..[75]]an upper limit on the aerosol concentration at that size. Thus, for every mode of the lognormal distribution, N_i represents the total number concentration, r_{mi} is the median radius, [..[76]]σ_{mi} is the mode width. [..[77]]The best fit is the distribution (BMLN or UMLN) which minimizes the sum over all measured sizes of the root mean square [..[78]]difference of the log of the fitted concentration and the log of the measured concentration. This method of searching for the best fitting parameters is quite similar to the chi-square technique described below, where here the use of logarithms provides the normalization by particle number concentration. Measurement uncertainties [..[79]]arise from variations of air sample flow rate, Poisson counting statistics, and the ability to duplicate the measurements from two identical instruments. [..[80]]The impact of these uncertainties on the size parameters have been approximated by a Monte Carlo simulation to be $\pm 30\%$ for size distribution parameters and $\pm 40\%$ for the aerosol moments (Deshler et al., 2003). A systematic calibration error affecting the counting efficiency of the instruments was described by Kovilakam and Deshler (2015). The discovery of this error has led to a modification in the fitting algorithm described in Deshler et al. (2003), such that now an explicit counting efficiency is included in the derivation of the lognormal size distribution fitting parameters [..[81]](Deshler et al., 2019), as indicated by CEF_{ch} in Equation (2).

[..[82]]During background stratospheric aerosol conditions, OPC measurements may not provide sufficient information about smaller particles ($r < 0.15$ µm) to determine a robust BMLN fit as shown in a recent study to improve OMPS/LP aerosol retrievals by Chen et al. (2018). In that study, Chen et al. (2018) compared four BMLN fits to the same OPC data at 20km altitude (made on 12 April 2000), all having a similar AE of approximately 2.4, but each with a different coarse mode fraction (CMF). These four BMLN distribution fits to the OPC data differed significantly from each other in the radius range between

[74] removed: or
[75] removed: the
[76] removed: and
[77] removed: $N(>r)$ is the concentration of all particles larger than the lower integration limit, r, and it is the quantity measured by the OPCs.
[78] removed: error with respect to the measurements (Deshler et al., 2003; Kovilakam and Deshler, 2015)
[79] removed: have been shown to produce errors associated with the variation
[80] removed: These uncertainties
[81] removed: (Deshler et al., 2018)
[82] removed: However, during

0.01μm to 0.1μm [..[83]](see Figure A1 of Chen et al., 2018), a region of the size distribution which is very challenging to measure with an OPC due to the small amount of light scattered by such small particles. These physical limitations on OPC measurements in turn limit the ability of the fits to be constrained. Consequently, the different ASDs produced $P_a(\Theta)$ that differed significantly [..[84]]from each other in backscatter as shown in Figure A2 of Chen et al. (2018). Additionally, the BMLN distribution, which is defined by 5 parameters (the CMF, 2 median radii, and 2 mode widths) that are independent of each other at each altitude, cannot generally be determined in cases where the measurements have less than 5 data points (Malinina et al., 2018). This [..[85]]limitation is further explored in the next section through [..[86]]a reexamination of the OPC data by fitting 2 single mode distributions to the concentration measurements and using only data available since 2008 that has a measurement between the 0.05 μm and 0.1 μm range.

3 Reanalysis of OPC size distribution fits

For a reanalysis of the OPC measurements, it was assumed the stratospheric aerosol could be described by a unimodal distribution during the non-volcanic period under consideration (2008-2017). Either a lognormal or a gamma model is used for which the number of degrees of freedom is reduced from five to two for a normalized distribution during the fitting process (described in Section 3.1). The normalization of the concentrations has no effect on the computation of the [..[87]]$P_a(\Theta)$ and the [..[88]]Ångström exponent for this study. The [..[89]]goodness of the fits is determined by the minimization of the chi-square (χ^2) test statistic. This method estimates the parameters of the fitted distribution by minimizing the difference between the hypothesized and observed distributions. If the data are grouped into k categories (i =1, 2, 3, ..., k) of radii size, the observed frequency in each class is denoted by O_i, and the expected probability from the hypothesized distribution by ζ_i, then the χ^2 value can be calculated from Equations (3[..[90]]) and (4), corresponding to Equation (5.14) described by Wilks (2011)

$$\chi^2(\xi) = \sum_{i=1}^{k} [..^{91}] \frac{[\frac{O_i}{n} - \zeta_i(\xi)]^2}{\zeta_i(\xi)} = \sum_{i=1}^{k} \frac{[O_i - n\zeta_i(\xi)]^2}{n^2\zeta_i(\xi)} \quad (3)$$

and

$$n = \sum_{i=1}^{k} O_i. \quad (4)$$

[83] removed: and these differences resulted from the gaps in the OPC size bins that limited
[84] removed: form each other
[85] removed: disparity
[86] removed: the
[87] removed: APF
[88] removed: A
[89] removed: choice of these two unimodal distributions is due to their similarity in appearance (Cho et al., 2004). The
[90] removed: and

To minimize the χ^2 value, the parameters (ξ) of the hypothesized distribution ζ are adjusted until the χ^2 value closest to zero is obtained (Cho et al., 2004). Thus, if the fitted distribution is closer to the distribution of the data, the expected number of particles and the observed number of the particles are very close for each radii range, and the square of the differences in the numerator of Equation (3) would be very small, leading to a small χ^2 (Wilks, 2011).

To assess whether the number of particles is being over or under estimated between the 0.05 µm and 0.1 µm radii range, data that includes a measurement within this range should be used, but such measurements are not [..[92]]generally available due to inherent limitations on the sensitivity of generic OPCs to particles less than 0.1 µm. Generally, the Wyoming in-situ OPC aerosol concentration measurements include [..[93]][..[94]]size resolved concentrations for particles [..[95]]between 0.15 µm and [..[96]]2.0 µm in 12 size classes. In addition, a second instrument is used to provide the concentration of all particles $>$ 0.01 µm using a condensation nuclei counter which provides no size information. Beginning in 2008 the OPC [..[97]]developed in the late 1980s (Hofmann and Deshler, 1991) was replaced with a new laser based OPC, or LPC (Ward et al., 2014), which is sensitive to particles from [..[98]]0.092 to 4.5 µm radius in 8 size classes. On certain occasions, between 2008 and 2010, there were measurements from both the older OPC and the newer LPC deployed on the same balloon. Further analysis and discussions will explore the importance of [..[99]]the additional bin at a radius of 0.092 µm by comparing the fits that include this bin [..[100]]to those that were fitted excluding this bin[..[101]], as well as the resulting phase functions derived from the fits in section 3.2.

3.1 Unimodal lognormal or gamma distribution

Aerosol concentration measurements from Laramie, Wyoming [..[102]]with the LPC are used for the current study because of the inclusion of a measurement between 0.05 µm and 0.1 µm. The LPC data consists of [..[103]]27 months of measurements as shown in Table 2 made from 2008 to 2017 that are fitted with the cumulative forms of the normalized UMLN distribution and the gamma distribution. These data are available from ftp://cat.uwyo.edu/pub/permanent/balloon/Aerosol_InSitu_Meas/US_Laramie_41N_105

[92] removed: always available
[93] removed: all particles whose radii are greater than 0.01
[94] removed: and
[95] removed: with radii greater than
[96] removed: typically up to
[97] removed: development
[98] removed: 0.094 to 2.0
[99] removed: this additional bin
[100] removed: (called LPC-like herein)
[101] removed: (called OPC-like herein)
[102] removed: that have been revised following (Kovilakam and Deshler, 2015; Deshler et al., 2018) and measurements
[103] removed: 20

The normalized form of the cumulative UMLN is obtained by setting N_i of Equation (2) to one and the [..[104]]cumulative gamma distribution is given by Equation (5).

$$F(x,\alpha,\beta) = \int_0^x f(u;\alpha,\beta)du \ = \frac{\gamma(\alpha,\beta,x)}{\Gamma(\alpha)} \tag{5}$$

In the case of the cumulative gamma distribution, $\gamma(\alpha,\beta,x)$ is the lower or incomplete gamma function, where α is the shape parameter and β is the rate parameter. The mean and variance of this distribution are respectively given by $\alpha\beta$ and $\alpha\beta^2$. This distribution can display many shapes by altering the values of α and β, and the pliable shape of this distribution makes it a good candidate for representing stratospheric aerosol data. A difficulty with this distribution, as stated by Wilks (2011), is that it is more tedious to work with the gamma distribution [..[105]]because the two parameters do not correspond exactly to physical parameters representative of the number size distribution of the sampled data, as is the case for the lognormal distribution.

Table 2. Table showing the year and the months on which the LPC data was included in this study. Each month represents one LPC flight with stratospheric measurements.

Year	Month
2008	October
2009	January June November
2010	March June
2011	March June July November
2012	January March May July September November
2013	March May August October
2014	March July September November
2015	January
2016	April
2017	November

The two altitudes, 20 km and 25 km are chosen to represent two differing aerosols loads well away from the tropopause. For the new fits, the measurements for each aerosol radius bin size which are reported as cumulative number concentrations (N_i) are first normalized to the total aerosol concentration N_0. This value represents the total number concentration and is obtained at the lowest integration limit of 0.01µm. After the normalization, bins that have quantities less than 1×10^{-6} cm^{-3} are omitted because this number is less than the smallest count distinguishable by the instrument used to make the measurements, which is $\sim 10^{-5}$ cm^{-3} (Deshler et al., 2003). The best fit (for which the χ^2 is minimized) is then chosen as the fit for that particular

[104]removed: cummulative
[105]removed: ,

distribution. Examples of the [..[106]]fitted cumulative UMLN and the gamma distributions to the OPC data for the two altitudes are shown in Figure 1 for the June 2010 data. [..[107]]The two ASDs tend to diverge beginning at radii greater than 300 nm and differ substantially at approximately 600 nm, where aerosol concentrations are below the minimum detectable concentrations, and there these differences can reach one order of magnitude. The figures also display for each fit the AE that was computed using Equation (1), where λ_1 and λ_2 are 525 nm and 1020 nm respectively.

To determine which of the two distributions was a better fit to the available data of each month's measurements, a statistical significance test was conducted by using the χ^2 goodness of fit test. This was done such that the null hypothesis H_o stated that: for each measurement the data [..[108]]were drawn from either a UMLN or a gamma distribution. The χ^2 is used as the test statistic with the degrees of freedom v given by Equation (6).

$$v = Number\ of\ measured\ bins - 2 - 1 \tag{6}$$

The number 2 in this equation represents the two parameters (r_m and σ, α and β, for the UMLN or the gamma, respectively) that are fitted for each distribution. The [..[109]]percentile value is defined as the distinct probability that the observed value of the test statistic will occur according to the null hypothesis. Subsequently, the null hypothesis is rejected if the percentile value is less than or equal to the test level and it is not rejected otherwise (Wilks, 2011). A complete summary of the percentile values computed for each of the two altitudes for all the data considered in comparing the two distributions is given in Figure 2. Results from this figure indicate that at both altitudes 20 km and 25 km, the null hypothesis is not rejected at the 15% test level (this corresponds to percentile values greater than 0.85). This signifies that at this level of significance [..[110]]the data could have been drawn from either a UMLN or gamma distribution. But at a 5% test level which corresponds to a percentile value greater than 0.95, the null hypothesis is rejected in favor of the alternate hypothesis that the data [..[111]]are taken from a UMLN distribution throughout the record at 25 km and for a majority of measurements at 20 km. Thus, the UMLN distribution is the better of the two distributions that were fitted to the data for the two altitudes that were used in this study.

The fitted parameters are then used to derive the phase functions which are compared among the two distributions. The phase functions derived from the parameters of both distributions compare well to within 10% of each other for scattering angles greater than 20°[..[112]]. Example of the [..[113]]derived phase functions for 675 nm [..[114]](wavelength used to perform aerosol extinction retrieval by OMPS V1.0) using the UMLN and the gamma distributions fitted parameters displayed in Figure 1 are shown in Figure 3. The shape of the phase functions has been observed to depend on magnitude of the median radius (r_m) in the case of the UMLN distribution and the shape parameter (α) in the case of the gamma distribution. As the

[106] removed: refitted
[107] removed: These
[108] removed: was
[109] removed: $percentile$
[110] removed: both the UMLN and the gamma distributions are good fits to the data, but
[111] removed: is taking
[112] removed: because the fits of the two distributions overlap
[113] removed: phase functions derived using the
[114] removed: wavelength

magnitude of these two parameters decreases, indicating smaller particles, the resulting phase functions produced from either of the distributions would more closely resemble a Rayleigh phase function[..[115]], as is suggested in Figure 3[..[116]], where the 25 km [..[117]]distribution (which has smaller particles) is compared to the 20 km[..[118]][..[119]], distribution (which has larger particles and hence larger values of r_m and α). Phase functions derived from the same dataset but using different fitting models differ from each other and this is a very important issue in the interpretation of measurements from scattering instruments. This is further compounded especially for limb scattering instruments due to multiple scattering effects, since [..[120]]differences in the phase functions produce reflectivity and altitude dependent [..[121]]differences in derived extinctions (Chen et al., 2018). Figure 3 also shows the range of scattering angles observed by OMPS-LP, SCIAMACHY and OSIRIS limb scattering satellite instruments.

The AE computed from the parameters of UMLN distribution fits to data are similar to those computed from the gamma distribution fitted parameters for the same altitude, as is shown in Figure 4. Moreover, a large AE corresponds to a small median radius in the case of the UMLN distribution or to a small shape parameter in the case of the gamma distribution.

[115] removed: as is shown by both distributions

[116] removed: for June 2010 altitude

[117] removed: when the parameters at this altitude are compared with those of June 2010 altitude

[118] removed: . Also, the overlapping behavior observed between the $P_a(\Theta)$ of each of the two distributions at both altitudes shown in Figure 3 is due to the inclusion of a measurement at ≈ 0.1

[119] removed: and its absence leads to large differences shown later

[120] removed: errors

[121] removed: errors

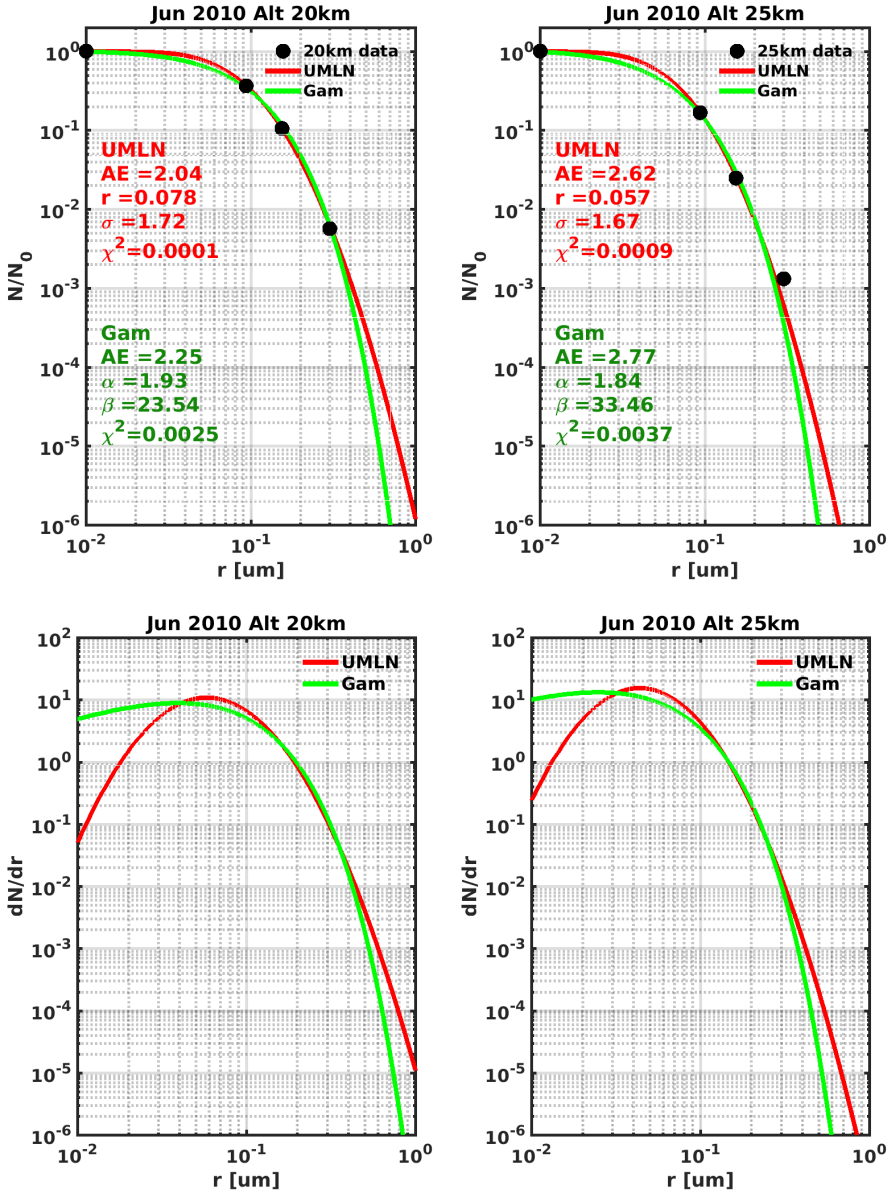

Figure 1. [..[122]]Topmost figures show examples of fitting the cumulative form of the UMLN (red line) and the gamma (green line) [..[123]]distributions to the June 2010 OPC data at altitudes 20 km (left) and 25 km (right) using the minimum χ^2 technique. The figures also show the results of each fit, the minimized χ^2 and the [..[124]]Ångström exponent derived from the fitted parameters. The figures at the bottom show the differential form of the two distributions.

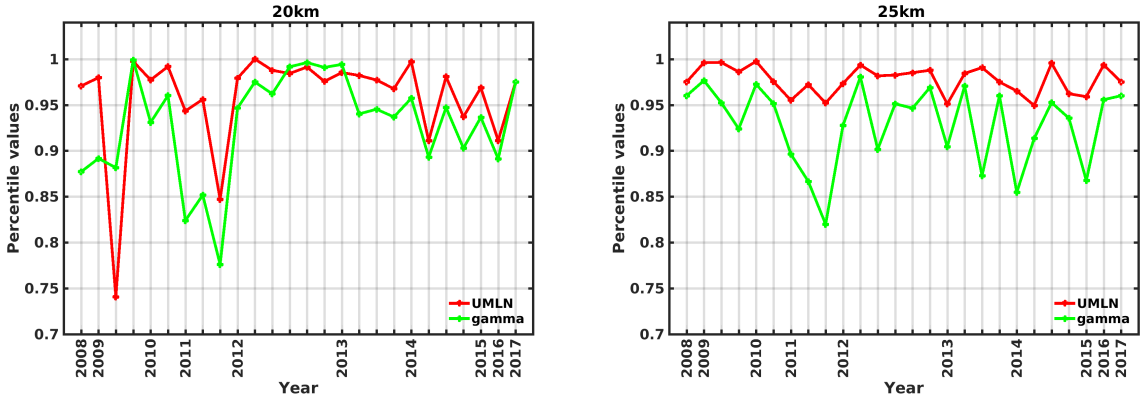

Figure 2. Percentile values computed for the χ^2 values of the UMLN (red line) and gamma (green line) distribution fits to 2008 to 2017 OPC data for altitudes 20 km (left) and 25 km (right).

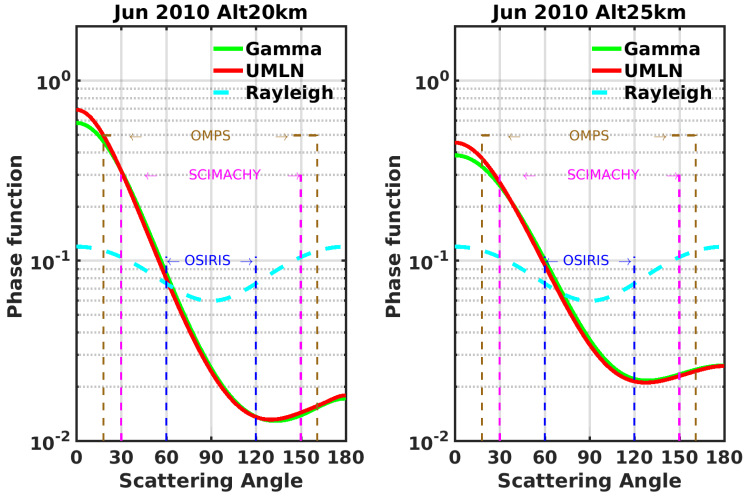

Figure 3. Phase functions derived at 675 nm using the fits shown in Figure 1 for June 2010. The figures correspond to altitude 20 km (left) and to altitude 25 km [..[125]](right). Also shown is the range of scattering angles for which aerosol extinctions are retrieved for OMPS, SCIAMACY and OSIRIS limb scatter instruments.

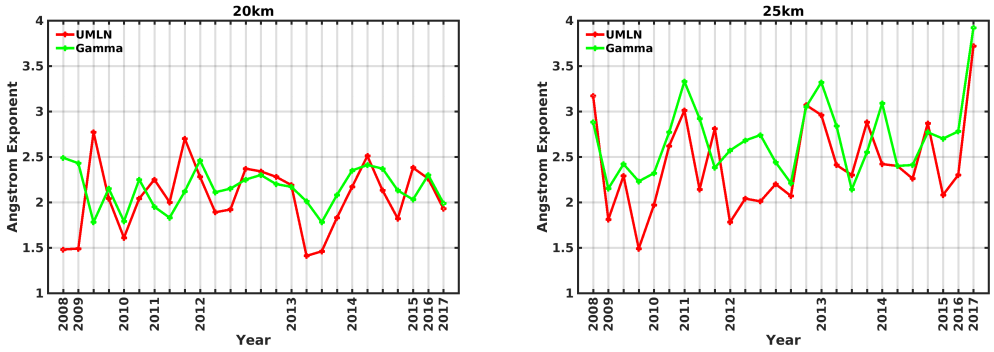

Figure 4. Computed [..[126]]Ångström exponents for both the UMLN (red lines) and the gamma (green lines) distribution at altitude 20 km(left) and 25 km (right). [..[127]]

3.2 Importance of a measurement between 0.05 µm and 0.1 µm

The form of $P_a(\Theta)$ for a particular aerosol is determined by the value of the size parameter X, which is the ratio of the aerosol circumference to the wavelength of interest ($X = \frac{2\pi r}{\lambda}$). [..[128]][..[129]][..[130]]Examples of phase functions for mono disperse aerosols for different X are shown in Figure 5[..[131]]. From this figure, the greatest sensitivity for the forward scattering angles of $P_a(\Theta)$ occurs when $X = 3$ and this implies an aerosol radius $r \approx 0.3$ µm for a wavelength of 675 nm. The phase function for $X = 3$ shows a forward peak and is nearly constant for scattering angles ($\Theta \geq 70°$). When there are no measurements between the 0.01 and 0.15 µm bin sizes, then the particle concentration within this range is estimated by the function used to fit the data. Errors in estimating the number of particles within this range by the function used for fitting the data will [..[132]]lead to uncertainties in the phase function [..[133]]as shown by the $X = 1$ plot in Figure 5. For an aerosol radius $r = 0.1$ µm, $P_a(\Theta)$ is approximately 30% greater than the Rayleigh phase function for scattering angles less than $60°$. The additional 0.092 µm bin in the LPC will augment the measurements.

[128] removed: OMPS V1 aerosol extinctions retrievals are done using the 0.675

[129] removed: wavelength, and so the phase function is particularly sensitive to aerosols with radius approximately 0.1

[130] removed: (making $X \approx 1$). This is

[131] removed: , where one observes a considerable change in the magnitude of the phase function, especially in the back-scattering directions ($\Theta \geq 90°$)for this X value

[132] removed: therefore

[133] removed: . The additional 0.094

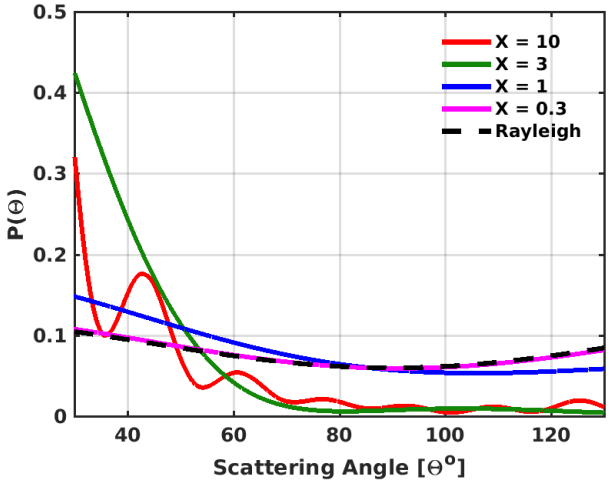

Figure 5. Mie phase functions of a monodisperse aerosol for different values of the size parameter X derived with a refractive index of 1.33. [..[134]]The increasing asymmetry and complexity (e.g. for X=10) of the phase functions with increasing X is due to the use of a monodisperse aerosol. The oscillations observed are damped when the phase functions are computed for an ensemble of aerosols that are assumed to have a UMLN or gamma distribution. The phase functions are shown for the range of scattering angles that are observed by OMPS, SCIAMACHY and OSIRIS.

[..[135]]The fits shown in Figure 1 are repeated for each of the two distributions, this time excluding the [..[136]]0.092 μm bin[..[137]]. These no small bin (nsb) fits are called UMLN$_{nsb}$ and gamma$_{nsb}$, and the resulting $P_a(\Theta)$ are compared at each altitude. A typical fit showing how the two distributions performed is shown in Figure 6 for June 2010 data at altitude 25 km. The topmost panels shown in Figure 6 indicate that [..[138]]the UMLN$_{nsb}$ distribution tends to underestimate the measured concentration at the [..[139]]0.092 μm bin position, whereas the same behavior is not seen with [..[140]][..[141]]gamma$_{nsb}$. These panels also show that only the UMLN$_{nsb}$ does a good job of fitting the 0.3 μm [..[142]]point, while both gamma distributions miss this point similar to UMLN. Also included in this figure are the [..[143]]$P_a(\Theta)$ (middle plots) determined for the 675 nm wavelength from the fitted parameters of both distributions[..[144]]. The range of scattering angles for which aerosol extinction retrievals are performed by OMPS, SCIAMACY and OSIRIS are indicated in this figure. The corresponding $P_a(\Theta)$ ratios

[135] removed: To show the differences that occur in the fitted distributions, the

[136] removed: 0.094

[137] removed: (to create an "OPC-like" fit) and comparing the phase functions

[138] removed: for the OPC-like fits, the UMLN

[139] removed: 0.094

[140] removed: the gammadistribution. The deviations between the fits of the UMLNdistribution tend to increase depending on where a measurement bin at the radius $r \approx 0.1$

[141] removed: of either the LPC-like or the OPC-like measurement is placed. Thus, the further away a measurement is positioned from $r = 0.1$

[142] removed: , the greater the differences observed in the UMLNdistribution fits

[143] removed: phase functions

[144] removed: and the corresponding phase function ratios (bottom plots) of the LPC-like and the OPC-like measurements

comparing the different fits are shown in the bottom plots. Changes of up to $\pm 30\%$ depending on the scattering angle are seen between the derived UMLN distribution [..[145]]$P_a(\Theta)$ comparison (UMLN/UMLN$_{nsb}$), whereas changes of up $\pm 10\%$ are observed for the derived gamma distribution [..[146]]$P_a(\Theta)$ comparison (Gam/Gam$_{nsb}$). The large differences between the UMLN $P_a(\Theta)$ and both UMLN$_{nsb}$ and gamma$_{nsb}$ is mainly due to the difference between the fits at 0.3 μm rather than particle radii less than 0.1 μm. Thus, underestimating the 0.3 μm data point leads to a reduction in the $P_a(\Theta)$ for the forward scattering angles and an increase in the phase function for the backward scattering angles. Also, since both gamma distributions underestimate the 0.3 μm point and are otherwise quite similar, their phase functions show very little variation due to the differences between the fits at 0.05 μm and 0.1 μm. Additionally, both UMLN and gamma distribution fits underestimated the particle radius at approximately 0.3 μm and a comparison of their phase functions (Gam/UMLN) show variations of $\pm 10\%$ for scattering angles greater than 30°. The failure of both gamma distributions to capture the OPC measurements for the largest bin size for the case shown in Figure 6 could lead to a systematic error in the derived phase functions.

The conclusion drawn from this comparison is that the phase functions calculated with the gamma distributions [..[147]][..[148]]with and without the small bin are comparable to each other to within 10% as compered to those of the UMLN distribution. This signifies [..[149]]that the gamma distribution is relatively insensitive to the addition of an intermediary bin between 0.05 μm and 0.1 μm, whereas the UMLN distribution is quite sensitive to this additional information.

[145] removed: phase functions comparison

[146] removed: phase function comparison.

[147] removed: are less sensitive to the radius $r \approx 0.1$

[148] removed: observation than the

[149] removed: the robustness of the gamma distribution when performing fits on measurements that are made without

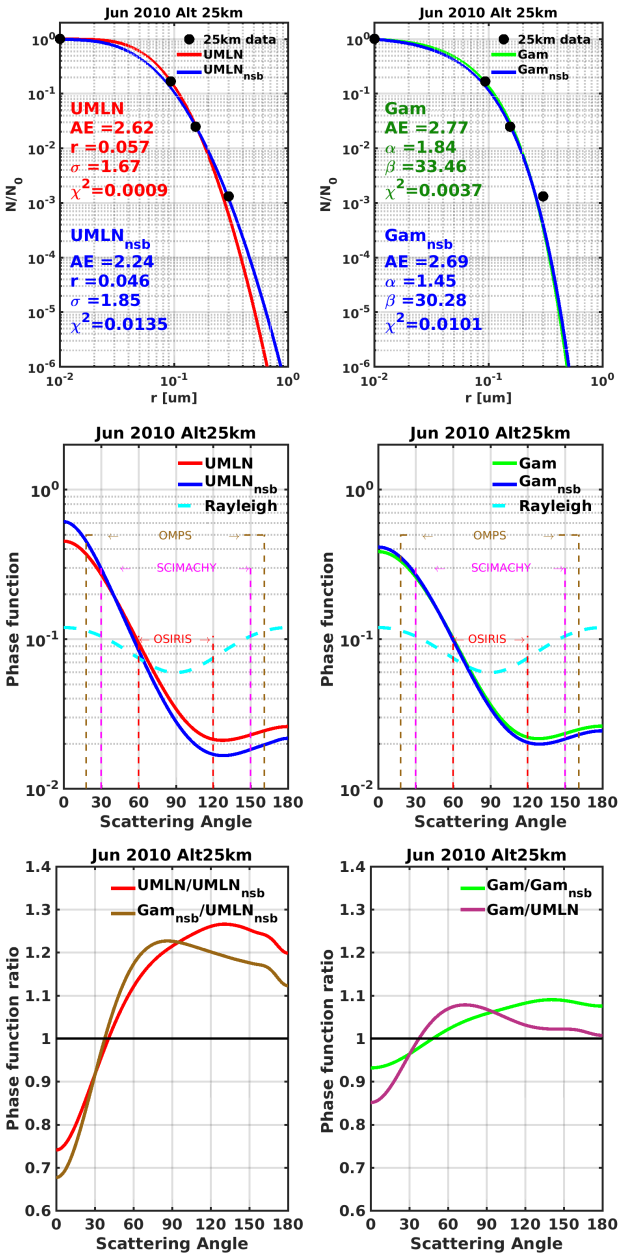

Figure 6. Unimodal lognormal distribution fits (top left) and gamma distribution (top right) fits to June 2010 data for altitude 25 km. Blue lines indicate fits$_{nsb}$ made without the 0.094 µm measurement[..[150]], while the red line fit includes all measurements as before ([..[151]]compare with Figure 1). The middle figures are the phase functions derived at 675 nm wavelength from the parameters of the fits. The range of scattering angles observed by OMPS, SCIAMACY and [..[152]]OSIRIS for which aerosol extinction retrievals are performed are also indicated on these figures. The bottom figures show the [..[153]]ratios of the phase functions of [..[154]]the different fits.

3.3 Comparison to the CARMA microphysical model results at Wyoming

The Community Aerosol and Radiation Model for Atmospheres (CARMA) is a general-purpose sectional microphysics code, which was derived from a one-dimensional stratospheric aerosol code that was developed by [..[155]]Turco et al. (1979); Toon et al. (1979, 1988) to study aerosols and clouds in planetary atmospheres (Hartwick and Toon, 2017). This model includes both aerosol microphysics and gas phase sulfur chemistry that has been described by [..[156]]English et al. (2011). CARMA has been implemented in the NASA Goddard Earth Observing System (GEOS) Earth system model (Rienecker et al., 2008; Colarco et al., 2014) and configured for modeling stratospheric aerosols similar to [..[157]]English et al. (2011). The ASD is not defined by a statistical distribution but instead is handled using a number of discrete size bins, where the model transport processes are allowed to affect each size bin independently [..[158]](Colarco et al., 2014). The $P_a(\Theta)$ produced by this model is computed directly using the outcome of each discrete bin to perform Mie calculations. The current configuration of this model employs 22 size bins ranging from [..[159]][..[160]]0.0002 µm to 2.79 µm at 72 vertical levels from the surface of the Earth up to 85 km. The distribution of the aerosol size bins is shown in Table 3. The model output for this comparison is the June-July-August (JJA) climatology that was averaged over 2008 to 2017 at Laramie, Wyoming. The atmosphere contains the background stratospheric aerosol layer, precursor emissions for anthropogenic sulfates, and degassing volcanoes that are not explosive in nature. The evolution of particles for this model arises from the nucleation of new sulfate particles, condensation of sulfuric acid [..[161]]vapor onto existing sulfate particles, and subsequent coagulation of sulfate particles. The cumulative UMLN size distribution and the cumulative gamma distribution are then fitted to the model results at [..[162]]altitudes between 19 and 26 km using Equations (2) and (5) respectively.

Table 3. Table shows the distribution of the 22 aerosol size bins for the radii of the particles employed in the CARMA model.

0.000267 µm	0.0004 µm	0.0006 µm	0.001 µm	0.0016 µm	0.002 µm	0.0038 µm	0.0058 µm
0.009 µm	0.014 µm	0.022 µm	0.034 µm	0.053 µm	0.082 µm	0.128 µm	0.198 µm
0.308 µm	0.479 µm	0.744 µm	1.156µm	1.796µm	2.79 µm		

The cumulative distributions fits are performed according to the methodology described in section 3.1 and using selected radii bins in conformity to the size resolved OPC measurements. The results are then validated using the information of all the model bin sizes within the 0.01 µm to 1 µm range. The fitted distributions on the model outputs are shown in Figure 7 for altitudes between 19 km and 26 km to include the two altitudes (20 and 25 km) that are being investigated because of the

[155] removed: (Turco et al., 1979; Toon et al., 1979, 1988)
[156] removed: (English et al., 2011)
[157] removed: English et al. (2011)
[158] removed: (Rienecker et al., 2008; Colarco et al., 2014). The APF
[159] removed: 0.2
[160] removed: to 3.25
[161] removed: into aerosols, coagulation and the uniform seeding of sulfuric acid gas
[162] removed: selected

irregular altitude grid employed in the GEOS model. Here, the minimized [..[163]]χ^2 of each fit are computed to include all the bins that were omitted during the fitting process. Comparing the magnitudes of the minimized χ^2 values between the two fitted distributions, the gamma distribution provides a better fit to the normalized CARMA model output at all altitudes that were considered in this study. Figure 7 illustrates the difficulties of a UMLN size distribution, which has the tendency to be too wide, and is one of the reasons why generally bimodal distributions have been found to do a better job in representing the OPC data (Deshler et al., 2003) when there are enough measurements. The gamma distribution does not have the same tendency to overestimate the larger particles. This is confirmed by performing a χ^2 statistic test as to which of these two distribution was a better fit to [..[164]]these model results. The [..[165]]computed percentile values [..[166]]shown in Figure 8 indicate that at each altitude considered, the gamma distribution is the best fit to the CARMA model results, within 15% at the outside. The relative differences (RD) computed as percentages using Equation (7) between the phase functions derived from the UMLN P_u and the gamma P_g fits [..[167]][..[168]][..[169]]are shown in Figure 9. This [..[170]]provides an indication of the differences that may occur in phase functions from using different size distributions across the range of scattering angles used by LS instruments.

$$RD\ (\%) = \left([..^{171}] \frac{P_g - P_u}{P_u} \right) \times 100\% \tag{7}$$

Finally, a comparison is made between the mean phase functions derived from OPC data fitted with the UMLN distribution and the CARMA model results fitted with the [..[172]]UMLN and gamma distributions at altitude 25 km. The mean and the standard deviation of OPC UMLN phase functions are obtained for each angle from the phase functions of all the months of June, July and August (JJA) from 2008 to 2017. Results from this comparison as shown in Figure 10 indicate that the phase function derived from the gamma distribution fit to the CARMA model outputs at Wyoming agrees very well to, within one standard deviation of, the mean phase function of the JJA UMLN distribution fit to the OPC dataset at this altitude. This agreement between the two phase functions is also shown to be within $\pm 15\%$ at all scattering angles and this reduces to $\pm 5\%$ within the scattering angle range of 15° to 180°. The phase functions derived from the CARMA model outputs using the UMLN distribution are also shown be within one standard deviation of the mean phase function of the JJA UMLN distribution fit to the OPC dataset at this altitude for all scattering angles greater than 15°. This corresponds to a $\pm 20\%$ change in the phase function for scattering angles greater than 15°. The good comparison shown by the phase [..[173]]functions derived from the CARMA model with that of the OPC dataset at Laramie, Wyoming[..[174]], provides evidence for

[163] removed: chi-squares
[164] removed: this
[165] removed: conclusion drawn from the
[166] removed: that are
[167] removed: show differences of up to $\pm 15\%$ at 19.85
[168] removed: to $\pm 50\%$ at 25.60
[169] removed: at different scattering angles as
[170] removed: implies that different distributions applied to the same data set would produce phase functions that differ greatly from each other at various scattering angles
[172] removed: gamma distribution
[173] removed: function
[174] removed: provides

the agreement of the CARMA model with the Wyoming OPC measurements and a justification for the use of the CARMA model results at other locations on the Earth and for periods with moderate volcanic activity.

The OMPS Version 1.5 (see Table 1) stratospheric aerosol extinction retrieval algorithm uses an ASD which is based on the gamma distribution function that has been derived from the CARMA model outputs at Laramie, Wyoming. Relative differences of the extinction profiles derived using this function and compared with collocated SAGE III (on the International Space Station) extinction profiles at 675 nm for the months of June to December 2017 have shown to be in agreement within generally less than 10% for altitudes 19 -29 km, with larger differences observed below 18 km due to uncertainties in the LP aerosol retrievals (see figure 12 of Chen et al. (2018)). The improvement observed in the aerosol extinction retrievals between the OMPS V1.0 and V1.5 is a source of motivation for a future OMPS/LP aerosol retrieval algorithm where the CARMA model results would be used to include the variation of the ASD and the $P_a(\Theta)$ with season, latitude, altitude and after a volcanic eruption. The current algorithm assumes that these properties do not vary with altitude and location (Chen et al., 2018).

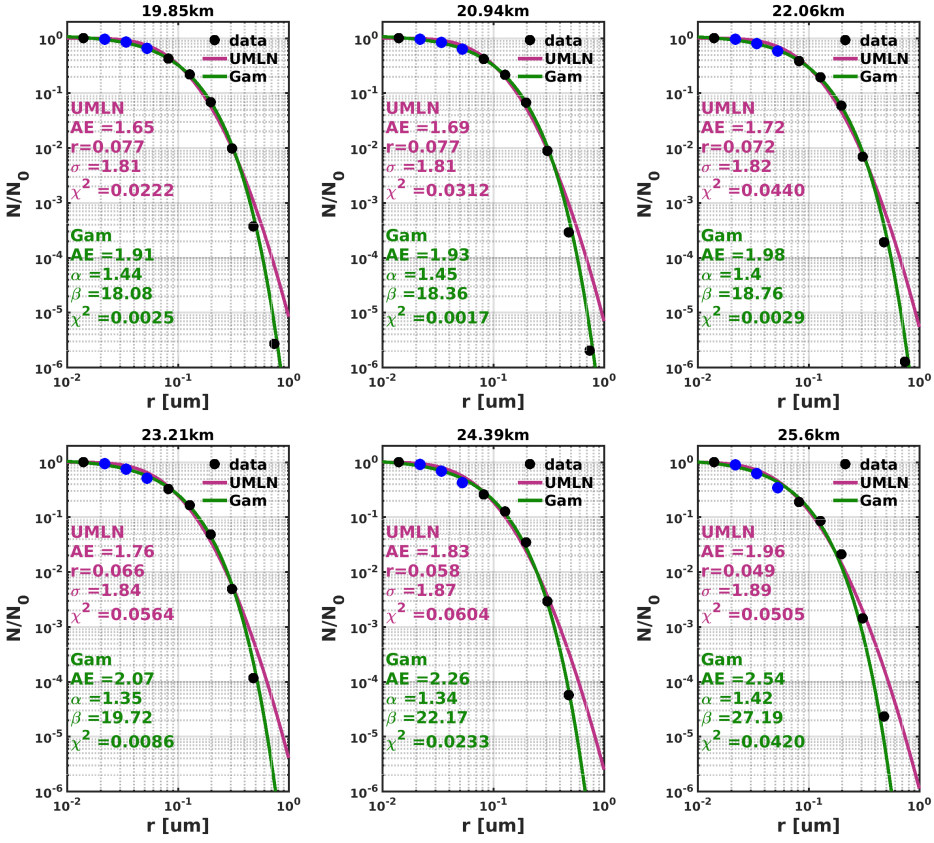

Figure 7. Unimodal lognormal and gamma distribution fits to the normalized CARMA model data. The blue data points are excluded during the fitting procedure, but are included during the validation of the fits. The green lines are the gamma distribution fits and the purple lines are the UMLN distribution fits.[..175]

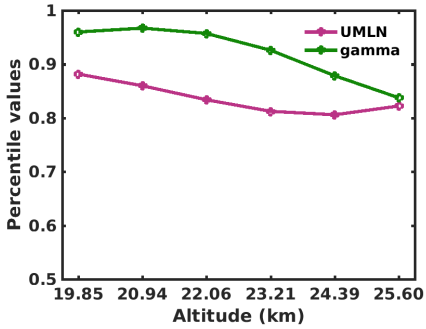

Figure 8. Percentile values computed from the minimized χ^2 of the fits of both the UMLN and gamma distributions to determine the level of confidence for which either distribution is chosen to describe the CARMA model data.

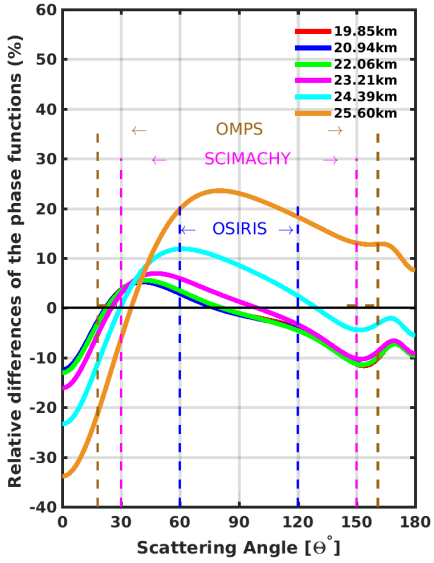

Figure 9. [..[176]]Relative differences between the [..[177]]phase functions derived from the gamma and the UMLN parameters fitted to the [..[178]]CARMA model data at each of the [..[179]]six altitudes from 19.85 km to 25.60 km.

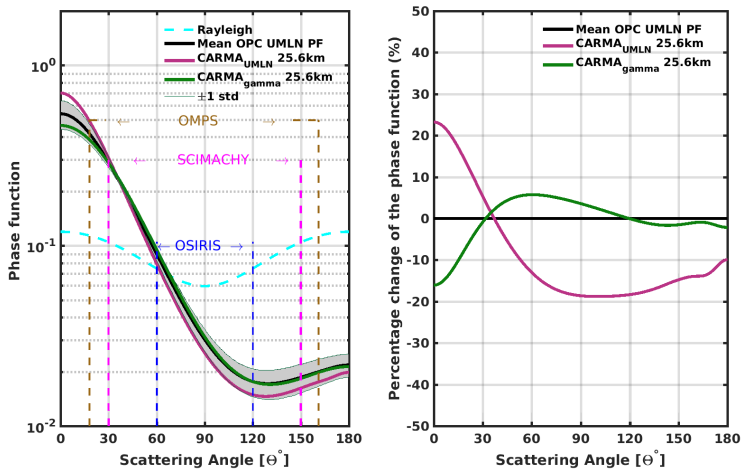

Figure 10. The figure on the left shows the mean and the standard deviation of phase functions, for the wavelength of 675 nm, derived from the fits of the UMLN distribution for all the OPC data used for the months of June, July and August (JJA) at altitude 25km [..[180]]compared to the phase [..[181]]functions derived from the [..[182]]UMLN and gamma fits to the CARMA model data at altitude 25.6 km[..[183]]. The figure on the right shows the [..[184]]percent changes between the [..[185]]UMLN derived phase functions [..[186]]from the OPC data and the UMLN and gamma derived phase functions from the CARMA model outputs.

4 Concluding discussions and Summary

Measured limb scattered radiance is sensitive to presence of stratospheric aerosols due to the long path the scattered solar photons have to travel through the aerosol layer to reach the sensor [..[187]](Rieger et al., 2015; Loughman et al., 2018; Chen et al., 2018). This radiance is [..[188]]composed of photons that were singly scattered directly [..[189]]along the line of sight (LOS) of the instrument [..[190]]and photons that were scattered multiple times before they were finally scattered into the LOS of the instrument. Along the LOS of the sensor, the scattered radiance [..[191]]arises from the aerosol phase function, $P_a(\Theta)$, but is attenuated by air molecules and trace gases, making untangling of the information content in these measurements very complicated. Moreover, diffuse upwelling radiation from the lower atmosphere is also scattered and attenuated along the LOS. To unravel the composition of these measurements requires a good knowledge of [..[192]]$P_a(\Theta)$ which is derived through the

[187] removed: (Loughman et al., 2018; Chen et al., 2018; Rieger et al., 2015)
[188] removed: not only
[189] removed: in the
[190] removed: but also includes
[191] removed: is driven not only by the APF but is further
[192] removed: APF

[..[193]]aerosol size distribution (ASD) that is assigned to these aerosols, and thus the choice of which theoretical distribution [..[194]]should be used to describe these particles in the stratosphere is important.

We have investigated fitting a [..[195]]unimodal lognormal (UMLN) and a gamma distribution to the 2008 to 2017 [..[196]]Wyoming in situ LPC measurements, which include a bin below 0.1 μm, for altitudes 20 km and 25 km. The parameters of the distributions were found by minimizing the χ^2 test statistic between the measurements and the theoretical distributions. As a first step, we assumed that the stratospheric aerosol is distributed with a single mode during the background conditions and could be fitted to either of the two distributions. Typically, both the UMLN and the gamma cumulative distributions are found to be good representatives for the stratospheric aerosol concentration measurements made by the University of Wyoming LPC at the two altitudes as was suggested by the χ^2 values. [..[197]]To discriminate between them, a χ^2 goodness of fit test applied showed that to a 10% level of confidence the UMLN was the better of the two distributions as it fitted all data at the two altitudes and for all the months of data that were considered.

Additionally, it has been shown that [..[198]]when the same LPC concentration measurements are [..[199]]fit without using the 0.092 μm bin, the gamma distribution [..[200]]provides a some what better fit because of its insensitivity to particles between 0.01 μm and 0.1 μm range when compared to the UMLN distribution[..[201]][..[202]][..[203]][..[204]]; however the gamma distribution in both cases underestimates the concentrations of the larger particles, which may be quite important depending on the wavelength of interest. This limited analysis [..[205]]suggests that when a single mode ASD [..[206]]was fitted to aerosol data that did not include sizes below 0.1 μm [..[207]]then the gamma distribution provided the better fit. When particle measurements below 0.1 μm were included, the UMLN distribution provided the better fit to the data.

A similar analysis was further conducted using data obtained from the aerosol microphysical model, CARMA to ascertain which distribution was the best to represent the background aerosol load in the stratosphere. Again, both distributions fitted these data very well for all the altitudes considered. Quantitative comparisons of the goodness of fit for these unimodal distributions indicated that the gamma distribution does a slightly better job for these comparisons in a volcanically quiescent

[193] removed: ASD
[194] removed: (UMLN or gamma)
[195] removed: UMLN
[196] removed: LPC measurements
[197] removed: In order to
[198] removed: whenever OPC-like
[199] removed: made
[200] removed: is the best distribution to be fitted to this data since it is more robust and able to predict the amount of particles within the
[201] removed: . This conclusion was drawn from the comparison of the phase functions derived from the two distributions fitted to the LPC data, when measurements are not provided between aerosol size ranges of 0.01
[202] removed: and 0.1
[203] removed: range by deliberately omitting the 0.094
[204] removed: bin and fitting the distributions
[205] removed: indicates that if
[206] removed: is to be assumed then the gamma distribution model provides an improved fit to the University of Wyoming LPC data , and by extension other in situ data, that do
[207] removed: in their measurements. When such small particle measurements are available, however, there is little distinction between the size distributions, if the usefulness of the physical significance of the lognormal size distribution parameters are not included

stratosphere. These kinds of closure studies are [..[208]]important for the improvement of [..[209]]confidence levels in space-based data that is used to test aerosol microphysical models and for estimating radiative forcing due to stratospheric aerosols.

The overall implication of this study is to show the importance of the nature of [..[210]]$P_a(\Theta)$ used in the retrieval of the stratospheric aerosol extinction from limb scattering measurements. [..[211]]Typically the phase function is derived from [..[212]]the parameters of [..[213]]a UMLN or a gamma distribution fitted to in situ data which may or may not include a measurement [..[214]][..[215]]below 0.1 µm [..[216]]radius. The work here shows the differences which can occur between fits made using a UMLN distribution and fits made [..[217]]using [..[218]]a gamma distribution. This leads to [..[219]]some disparity in the phase functions used to represent the measurements. Thus, it is imperative for one to have a knowledge about the nature of the measurements from which the parameters of any distribution are provided. [..[220]][..[221]][..[222]]

Data availability. OPC data are available for download at: ftp://cat.uwyo.edu/pub/permanent/balloon/Aerosol_InSitu_Meas/US_Laramie_41N_105W/.

Competing interests. The authors declare that they have no conflict of interest.

Acknowledgements. This work was supported by NASA GSFC through SSAI Subcontract 21205-12-043. The Wyoming in situ data are collected through support from NSF under awards: 0538679, 1011827, 1619632. The authors thank NASA and NOAA for supporting limb scattering research, and particularly recognize Didier Rault for years of leadership developing the OMPS LP algorithms. We would also like to thank Matthew DeLand for his support.

[208] removed: very
[209] removed: the
[210] removed: APF
[211] removed: The
[212] removed: either
[213] removed: the UMLN or the gamma cumulative distributions fitted to LPC measurements and other
[214] removed: in the aerosol size range of 0.01
[215] removed: and
[216] removed: . The
[217] removed: by using the UMLN distribution have a tendency to over or under estimate the number of particles within this aerosol size range as compared to fits made
[218] removed: the gamma distributionwhen no measurements are given within that radii range
[219] removed: phase functions that may not be a true representation of
[220] removed: Because of the robustness of the gamma distribution, phase functions are best computed with this distribution for in situ or OPC measurements that do not provide a data point in the aerosol size range of 0.01
[221] removed: and 0.1
[222] removed: .

References

Andreae, M. O. and Crutzen, P. J.: Atmospheric aerosols: Biogeochemical sources and role in atmospheric chemistry, Science, 276, 1052–1058, 1997.

Ångström, A.: On the atmospheric transmission of sun radiation and on dust in the air, Geografiska Annaler, 11, 156–166, 1929.

Berthet, G., Jégou, F., Catoire, V., Krysztofiak, G., Renard, J.-B., Bourassa, A. E., Degenstein, D. A., Brogniez, C., Dorf, M., Kreycy, S., et al.: Impact of a moderate volcanic eruption on chemistry in the lower stratosphere: balloon-borne observations and model calculations, Atmospheric Chemistry and Physics, 17, 2229–2253, 2017.

Boucher, O.: On aerosol direct shortwave forcing and the Henyey-Greenstein phase function, Journal of the atmospheric sciences, 55, 128–134, 1998.

Bourassa, A., Degenstein, D., and Llewellyn, E.: Retrieval of stratospheric aerosol size information from OSIRIS limb scattered sunlight spectra, Atmospheric Chemistry and Physics, 8, 6375–6380, 2008.

Bourassa, A. E., Degenstein, D. A., Gattinger, R. L., and Llewellyn, E. J.: Stratospheric aerosol retrieval with optical spectrograph and infrared imaging system limb scatter measurements, Journal of Geophysical Research D: Atmospheres, 112, 2007.

Bourassa, A. E., Rieger, L. A., Lloyd, N. D., and Degenstein, D. A.: Odin-OSIRIS stratospheric aerosol data product and SAGE III intercomparison, Atmospheric Chemistry and Physics, 12, 605–614, https://doi.org/10.5194/acp-12-605-2012, https://www.atmos-chem-phys.net/12/605/2012/, 2012.

Bovensmann, H., Burrows, J., Buchwitz, M., Frerick, J., Noël, S., Rozanov, V., Chance, K., and Goede, A.: SCIAMACHY: Mission objectives and measurement modes, Journal of the Atmospheric Sciences, 56, 127–150, 1999.

Campbell, P. and Deshler, T.: Condensation nuclei measurements in the midlatitude (1982–2012) and Antarctic (1986–2010) stratosphere between 20 and 35 km, Journal of Geophysical Research: Atmospheres, 119, 137–152, 2014.

Chen, Z., Bhartia, P. K., Loughman, R., Colarco, P., and DeLand, M.: Improvement of stratospheric aerosol extinction retrieval from OMPS/LP using a new aerosol model, Atmospheric Measurement Techniques, 11, 6495–6509, 2018.

Cho, H.-K., Bowman, K. P., and North, G. R.: A comparison of gamma and lognormal distributions for characterizing satellite rain rates from the tropical rainfall measuring mission, Journal of Applied Meteorology, 43, 1586–1597, 2004.

Colarco, P. R., Nowottnick, E. P., Randles, C. A., Yi, B., Yang, P., Kim, K.-M., Smith, J. A., and Bardeen, C. G.: Impact of radiatively interactive dust aerosols in the NASA GEOS-5 climate model: Sensitivity to dust particle shape and refractive index, Journal of Geophysical Research: Atmospheres, 119, 753–786, https://doi.org/10.1002/2013JD020046, 2014.

Cornette, W. M. and Shanks, J. G.: Physically reasonable analytic expression for the single-scattering phase function, Applied optics, 31, 3152–3160, 1992.

Davies, C.: Size distribution of atmospheric particles, Journal of Aerosol Science, 5, 293 – 300, https://doi.org/https://doi.org/10.1016/0021-8502(74)90063-9, http://www.sciencedirect.com/science/article/pii/0021850274900639, 1974.

Deepak, A. and Box, G. P.: Representation of aerosol size distribution data by analytic models, in: Atmospheric Aerosols: Their Formation, Optical Properties, and Effects, p. 79, 1982.

Deirmendjian, D.: Electromagnetic scattering on spherical polydispersions, Tech. rep., RAND CORP SANTA MONICA CA, 1969.

DeLand, M., Bhartia, P., Xu, P., and Zhu, T.: OMPS Limb Profiler Aerosol Extinction Product AER675: Version 0.5 Data Release Notes, https://ozoneaq.gsfc.nasa.gov/media/docs/OMPS_LP_AER675_V0.5_Release_Notes.pdf, 2016.

Deshler, T., Johnson, B. J., and Rozier, W. R.: Balloonborne measurements of Pinatubo aerosol during 1991 and 1992 at 41°N: Vertical profiles, size distribution, and volatility, Geophysical Research Letters, 20, 1435–1438, https://doi.org/10.1029/93GL01337, http://dx.doi.org/10.1029/93GL01337, 1993.

Deshler, T., Hervig, M., Hofmann, D., Rosen, J., and Liley, J.: Thirty years of in situ stratospheric aerosol size distribution measurements from Laramie, Wyoming (41 N), using balloon-borne instruments, Journal of Geophysical Research: Atmospheres, 108, 2003.

Deshler, T., Kovilakam, M., Luo, B., Peter, T., and Kalnajs, L.: Retrieval of aerosol size distributions from in situ particle counter measurements accounting for instrument counting efficiency, and comparisons with satellite measurements of extinction and estimates of aerosol surface area, Submitted to Journal of Geophysical Research, 2018.

Deshler, T., Luo, B., Kovilakam, M., Peter, T., and Kalnajs, L. E.: Retrieval of Aerosol Size Distributions From In Situ Particle Counter Measurements: Instrument Counting Efficiency and Comparisons With Satellite Measurements, Journal of Geophysical Research: Atmospheres, 124, 5058–5087, 2019.

English, J., Toon, O., Mills, M., and Yu, F.: Microphysical simulations of new particle formation in the upper troposphere and lower stratosphere, Atmospheric Chemistry and Physics, 11, 9303, 2011.

Ernst, F.: Stratospheric aerosol extinction profile retrievals from SCIAMACHY limb-scatter observations, Ph.D. thesis, Staats-und Universitätsbibliothek Bremen, 2013.

Flynn, L., Seftor, C., Larsen, J., and Xu, P.: The Ozone Mapping and Profiler Suite, in: Earth Science Satellite Remote Sensing, edited by Qu, J., Gao, W., Kafatos, M., Murphy, R., and Salomonson, V., pp. 279–296, Springer Berlin Heidelberg, https://doi.org/10.1007/978-3-540-37293-6_15, http://dx.doi.org/10.1007/978-3-540-37293-6_15, 2006.

Fromm, M., Lindsey, D. T., Servranckx, R., Yue, G., Trickl, T., Sica, R., Doucet, P., and Godin-Beekmann, S.: The untold story of pyrocumulonimbus, bulletin of the american meteorological Society, 91, 1193–1209, 2010.

Grams, G. W.: In-situ measurements of scattering phase functions of stratospheric aerosol particles in Alaska during July 1979, Geophysical Research Letters, 8, 13–14, https://doi.org/10.1029/GL008i001p00013, https://agupubs.onlinelibrary.wiley.com/doi/abs/10.1029/GL008i001p00013, 1981.

Hamill, P., Jensen, E. J., Russell, P., and Bauman, J. J.: The life cycle of stratospheric aerosol particles, Bulletin of the American Meteorological Society, 78, 1395–1410, 1997.

Hartwick, V. and Toon, O.: Micrometeoric Ablation Biproducts as a High Altitude Source for Ice Nuclei in the Present Day Martian Atmosphere, in: The Sixth International Workshop on the Mars Atmosphere: Modelling and observation was held on January 17-20 2017, in Granada, Spain. Scientific committee: F. Forget, MA Lopez-Valverde, S. Amiri, M.-C. Desjean, F. Gonzalez-Galindo, J. Hollingsworth, B. Jakosky, SR Lewis, D. McCleese, E. Millour, H. Svedhem, D. Titov, M. Wolff., p. 4103, p. 4103, 2017.

Henyey, L. G. and Greenstein, J. L.: Diffuse radiation in the galaxy, The Astrophysical Journal, 93, 70–83, 1941.

Hinds, W.: Aerosol technology: properties, behavior, and measurement of airborne particles, A Wiley-Interscience Publication John Wiley & Sons, 1982.

Hofmann, D. and Deshler, T.: Stratospheric cloud observations during formation of the Antarctic ozone hole in 1989, Journal of Geophysical Research: Atmospheres, 96, 2897–2912, 1991.

Horvath, H., Gunter, R., and Wilkison, S.: Determination of the coarse mode of the atmospheric aerosol using data from a forward-scattering spectrometer probe, Aerosol Science and Technology, 12, 964–980, 1990.

Irvine, W. M.: Multiple Scattering by Large Particles., The Astrophysical Journal, 142, 1563, 1965.

Ivy, D. J., Solomon, S., Kinnison, D., Mills, M. J., Schmidt, A., and Neely, R. R.: The influence of the Calbuco eruption on the 2015 Antarctic ozone hole in a fully coupled chemistry-climate model, Geophysical Research Letters, 44, 2556–2561, 2017.

Jaross, G., Bhartia, P. K., Chen, G., Kowitt, M., Haken, M., Chen, Z., Xu, P., Warner, J., and Kelly, T.: OMPS Limb Profiler instrument performance assessment, Journal of Geophysical Research: Atmospheres, 119, 4399–4412, 2014.

Junge, C. E.: Air chemistry and radioactivity, 1963, p. 382, 1963.

Junge, C. E., Chagnon, C. W., and Manson, J. E.: A world-wide stratospheric aerosol layer, Science, 133, 1478–1479, 1961.

Khaykin, S., Godin-Beekmann, S., Hauchecorne, A., Pelon, J., Ravetta, F., and Keckhut, P.: Stratospheric smoke with unprecedentedly high backscatter observed by lidars above southern France, Geophysical Research Letters, 45, 1639–1646, 2018.

Kovilakam, M. and Deshler, T.: On the accuracy of stratospheric aerosol extinction derived from in situ size distribution measurements and surface area density derived from remote SAGE II and HALOE extinction measurements, Journal of Geophysical Research: Atmospheres, 120, 8426–8447, 2015.

Kravitz, B., Robock, A., Bourassa, A., Deshler, T., Wu, D., Mattis, I., Finger, F., Hoffmann, A., Ritter, C., Bitar, L., et al.: Simulation and observations of stratospheric aerosols from the 2009 Sarychev volcanic eruption, Journal of Geophysical Research: Atmospheres, 116, 2011.

Kremser, S., Thomason, L. W., Hobe, M., Hermann, M., Deshler, T., Timmreck, C., Toohey, M., Stenke, A., Schwarz, J. P., Weigel, R., et al.: Stratospheric aerosol—Observations, processes, and impact on climate, Reviews of Geophysics, 54, 278–335, 2016.

Llewellyn, E. J., Lloyd, N. D., Degenstein, D. A., Gattinger, R. L., Petelina, S. V., Bourassa, A. E., Wiensz, J. T., Ivanov, E. V., McDade, I. C., Solheim, B. H., McConnell, J. C., Haley, C. S., Von Savigny, C., Sioris, C. E., McLinden, C. A., Griffioen, E., Kaminski, J., Evans, W. F. J., Puckrin, E., Strong, K., Wehrle, V., Hum, R. H., Kendall, D. J. W., Matsushita, J., Murtagh, D. P., Brohede, S., Stegman, J., Witt, G., Barnes, G., Payne, W. F., Piché, L., Smith, K., Warshaw, G., Deslauniers, D. ., Marchand, P., Richardson, E. H., King, R. A., Wevers, I., McCreath, W., Kyrölä, E., Oikarinen, L., Leppelmeier, G. W., Auvinen, H., Mégie, G., Hauchecorne, A., Lefèvre, F., De La Nöe, J., Ricaud, P., Frisk, U., Sjoberg, F., Von Schéele, F., and Nordh, L.: The OSIRIS instrument on the Odin spacecraft, Canadian Journal of Physics, 82, 411–422, 2004.

Loughman, R., Flittner, D., Nyaku, E., and Bhartia, P. K.: Gauss-Seidel limb scattering (GSLS) radiative transfer model development in support of the Ozone Mapping and Profiler Suite (OMPS) limb profiler mission, Atmospheric Chemistry and Physics, 15, 3007–3020, http://www.atmos-chem-phys.net/15/3007/2015/, 2015.

Loughman, R., Bhartia, P. K., Chen, Z., Xu, P., Nyaku, E., and Taha, G.: The Ozone Mapping and Profiler Suite (OMPS) Limb Profiler (LP) Version 1 aerosol extinction retrieval algorithm: theoretical basis, Atmospheric Measurement Techniques, 11, 2633–2651, https://doi.org/10.5194/amt-11-2633-2018, https://www.atmos-meas-tech.net/11/2633/2018/, 2018.

Malinina, E., Rozanov, A., Rozanov, V., Liebing, P., Bovensmann, H., and Burrows, J. P.: Aerosol particle size distribution in the stratosphere retrieved from SCIAMACHY limb measurements, Atmospheric Measurement Techniques, 11, 2085–2100, 2018.

McCormick, M. P. and Veiga, R. E.: SAGE II measurements of early Pinatubo aerosols, Geophysical Research Letters, 19, 155–158, 1992.

McCormick, M. P., Thomason, L. W., and Trepte, C. R.: Atmospheric effects of the Mt Pinatubo eruption, Nature, 373, 399–404, 1995.

Mie, G.: Beiträge zur Optik trüber Medien, speziell kolloidaler Metallösungen, Annalen der Physik, 330, 377–445, https://doi.org/10.1002/andp.19083300302, 1908.

Nyaku, E. M.: Characterizing aerosol properties in the upper troposphere and stratosphere from limb scatter radiance, PhD dissertation, Hampton University, Center for Atmospheric Sciences, this is a full PHDTHESIS entry, 2016.

Ovigneur, B., Landgraf, J., Snel, R., and Aben, I.: Retrieval of stratospheric aerosol density profiles from SCIAMACHY limb radiance measurements in the O 2 A-band, Atmospheric Measurement Techniques, 4, 2359–2373, 2011.

Palmer, K. F. and Williams, D.: Optical constants of sulfuric acid; application to the clouds of Venus?, Applied Optics, 14, 208–219, 1975.

Randel, W. J., Park, M., Emmons, L., Kinnison, D., Bernath, P., Walker, K. A., Boone, C., and Pumphrey, H.: Asian monsoon transport of pollution to the stratosphere, Science, 328, 611–613, 2010.

Rault, D. and Loughman, R.: Stratospheric and upper tropospheric aerosol retrieval from limb scatter signals, in: Proc. SPIE, vol. 6745, p. 674509, 2007.

Rault, D. F. and Loughman, R. P.: The OMPS limb profiler environmental data record algorithm theoretical basis document and expected performance, IEEE Transactions on Geoscience and Remote Sensing, 51, 2505–2527, 2013.

Ridley, D., Solomon, S., Barnes, J., Burlakov, V., Deshler, T., Dolgii, S., Herber, A. B., Nagai, T., Neely, R., Nevzorov, A., et al.: Total volcanic stratospheric aerosol optical depths and implications for global climate change, Geophysical Research Letters, 41, 7763–7769, 2014.

Rieger, L., Bourassa, A., and Degenstein, D.: Merging the OSIRIS and SAGE II stratospheric aerosol records, Journal of Geophysical Research: Atmospheres, 120, 8890–8904, 2015.

Rieger, L. A., Bourassa, A. E., and Degenstein, D. A.: Stratospheric aerosol particle size information in Odin-OSIRIS limb scatter spectra, Atmospheric Measurement Techniques, 7, 507–522, https://doi.org/10.5194/amt-7-507-2014, http://www.atmos-meas-tech.net/7/507/2014/, 2014.

Rieger, L. A., Malinina, E. P., Rozanov, A. V., Burrows, J. P., Bourassa, A. E., and Degenstein, D. A.: A study of the approaches used to retrieve aerosol extinction, as applied to limb observations made by OSIRIS and SCIAMACHY, Atmospheric Measurement Techniques, 11, 3433–3445, https://doi.org/10.5194/amt-11-3433-2018, https://www.atmos-meas-tech.net/11/3433/2018/, 2018.

Rienecker, M., Suarez, M. J., Todling, R., Bacmeister, J., Takacs, L., Liu, H., Gu, W., Sienkiewicz, M., Koster, R., Gelaro, R., Stajner, I., and Nielsen, J.: The GEOS-5 Data Assimilation System-Documentation of Versions 5.0. 1, 5.1. 0, and 5.2. 0, NASA Technical Report Series on Global Modeling and Data Assimilation, 27, 1–118, 2008.

Robock, A.: Volcanic eruptions and climate, Reviews of Geophysics, 38, 191–219, 2000.

Rosen, J. M.: The vertical distribution of dust to 30 kilometers, Journal of Geophysical Research, 69, 4673–4676, https://doi.org/10.1029/JZ069i021p04673, http://dx.doi.org/10.1029/JZ069i021p04673, 1964.

Rosen, J. M. and Hofmann, D. J.: Optical modeling of stratopheric aerosols: present status, Applied optics, 25, 410–419, 1986.

Russell, P. B. and McCormick, M. P.: SAGE II aerosol data validation and initial data use: an introduction and overview, Journal of Geophysical Research, 94, 8335–8338, 1989.

Schuster, G. L., Dubovik, O., and Holben, B. N.: Ångström exponent and bimodal aerosol size distributions, Journal of Geophysical Research: Atmospheres, 111, 2006.

Solomon, S.: Stratospheric ozone depletion: A review of concepts and history, Reviews of Geophysics, 37, 275–316, 1999.

SPARC: SPARC Assessment of Stratospheric Aerosol Properties, L. Thomason and T. Peter (eds.), SPARC Report No. 4, 2006.

Steele, H. M. and Turco, R. P.: Retrieval of aerosol size distributions from satellite extinction spectra using constrained linear inversion, Journal of Geophysical Research: Atmospheres, 102, 16 737–16 747, https://doi.org/10.1029/97JD01264, http://dx.doi.org/10.1029/97JD01264, 1997.

Taha, G., Rault, D. F., Loughman, R. P., Bourassa, A. E., and Von Savigny, C.: SCIAMACHY stratospheric aerosol extinction profile retrieval using the OMPS/LP algorithm, Atmospheric Measurement Techniques, 4, 547–556, 2011.

Thomason, L., Poole, L., and Deshler, T.: A global climatology of stratospheric aerosol surface area density deduced from Stratospheric Aerosol and Gas Experiment II measurements: 1984–1994, Journal of Geophysical Research: Atmospheres, 102, 8967–8976, 1997.

Thomason, L. W., Burton, S. P., Luo, B.-P., and Peter, T.: SAGE II measurements of stratospheric aerosol properties at non-volcanic levels, Atmospheric Chemistry and Physics, 8, 983–995, 2008.

Toon, O., Turco, R., Westphal, D., Malone, R., and Liu, M.: A multidimensional model for aerosols: Description of computational analogs, Journal of the Atmospheric Sciences, 45, 2123–2144, 1988.

Toon, O. B. and Pollack, J. B.: A global average model of atmospheric aerosols for radiative transfer calculations, Journal of Applied Meteorology, 15, 225–246, 1976.

Toon, O. B., Turco, R., Hamill, P., Kiang, C., and Whitten, R.: A one-dimensional model describing aerosol formation and evolution in the stratosphere: II. Sensitivity studies and comparison with observations, Journal of the Atmospheric Sciences, 36, 718–736, 1979.

Toublanc, D.: Henyey–Greenstein and Mie phase functions in Monte Carlo radiative transfer computations, Applied optics, 35, 3270–3274, 1996.

Turco, R., Hamill, P., Toon, O., Whitten, R., and Kiang, C.: A one-dimensional model describing aerosol formation and evolution in the stratosphere: I. Physical processes and mathematical analogs, Journal of the Atmospheric Sciences, 36, 699–717, 1979.

Vernier, J.-P., Thomason, L. W., Pommereau, J.-P., Bourassa, A., Pelon, J., Garnier, A., Hauchecorne, A., Blanot, L., Trepte, C., Degenstein, D., et al.: Major influence of tropical volcanic eruptions on the stratospheric aerosol layer during the last decade, Geophysical Research Letters, 38, 2011.

von Savigny, C., Ernst, F., Rozanov, A., Hommel, R., Eichmann, K.-U., Rozanov, V., Burrows, J. P., and Thomason, L. W.: Improved stratospheric aerosol extinction profiles from SCIAMACHY: validation and sample results, Atmospheric Measurement Techniques, 8, 5223–5235, https://doi.org/10.5194/amt-8-5223-2015, http://www.atmos-meas-tech.net/8/5223/2015/, 2015.

Ward, S. M., Deshler, T., and Hertzog, A.: Quasi-Lagrangian measurements of nitric acid trihydrate formation over Antarctica, Journal of Geophysical Research: Atmospheres, 119, 245–258, https://doi.org/10.1002/2013JD020326, http://dx.doi.org/10.1002/2013JD020326, 2013JD020326, 2014.

Wilks, D.: Statistical Methods in the Atmospheric Sciences, vol. 100, Academic Press, 3 edn., 2011.

Yue, G. K.: A new approach to retrieval of aerosol size distributions and integral properties from SAGE II aerosol extinction spectra, Journal of Geophysical Research: Atmospheres, 104, 27 491–27 506, 1999.